



**Convolution models  
revisited**

S. Seeger and M. Weiler

This discussion paper is/has been under review for the journal Hydrology and Earth System Sciences (HESS). Please refer to the corresponding final paper in HESS if available.

# Lumped convolution integral models revisited: on the meaningfulness of inter catchment comparisons

**S. Seeger and M. Weiler**

Albert-Ludwigs-University of Freiburg, Freiburg, Germany

Received: 26 May 2014 – Accepted: 2 June 2014 – Published: 24 June 2014

Correspondence to: S. Seeger (stefan.seeger@hydrology.uni-freiburg.de)

Published by Copernicus Publications on behalf of the European Geosciences Union.

[Title Page](#)

<a href="#">Abstract</a>	<a href="#">Introduction</a>
<a href="#">Conclusions</a>	<a href="#">References</a>
<a href="#">Tables</a>	<a href="#">Figures</a>

[|◀](#) [▶|](#)

[◀](#) [▶](#)

[Back](#) [Close](#)

[Full Screen / Esc](#)

[Printer-friendly Version](#)

[Interactive Discussion](#)



## Abstract

The transit time distribution of a catchment is linked to the water storage potential and affects the susceptibility of a catchment to pollution. However, this characteristic of a catchment is still problematic to determine within a catchment and to predict among catchments based on physiographic or geological properties. In this study, lumped response and transit time convolution models coupled with a distributed physically based snow model were applied to simulate the stable water isotope compositions in stream discharge measured fortnightly in 24 meso-scale catchments in Switzerland. Three different types of transfer function (exponential, gamma distribution and two parallel linear reservoirs) in two different implementation variants (strictly mathematical and normalised) were optimised and compared. The derived mean transit times varied widely for one and the same catchment depending on the chosen transfer function, even when the model simulations led to very similar predictions of the tracer signal. Upon closer inspection of the transit time distributions, it appeared that two transfer functions mainly have to agree on an intermediate time scale around three months to reach similarly good prediction results in respect to fortnightly discharge samples, while their short-term and long-term behaviour seem to be of minor importance for the evaluation of the models. A couple of topographic indices showed significant correlations with the derived mean transit times. However, the collinearity of those indices, which were also correlated to mean annual precipitation sums, and the differing results among the different transfer functions, did not allow for the clear identification of one predictive topographical index. As a by-product of this study, a spatial interpolation method for monthly isotope concentrations in precipitation with modest input data requirement was developed and tested.

## HESSD

11, 6753–6803, 2014

### Convolution models revisited

S. Seeger and M. Weiler

Title Page

Abstract

Introduction

Conclusions

References

Tables

Figures

⏪

⏩

◀

▶

Back

Close

Full Screen / Esc

Printer-friendly Version

Interactive Discussion



# 1 Introduction

Stable water isotopes or other natural constituents, like chloride, in precipitation act as environmental tracers whose signals are altered by hydrological processes, storage and mixing inside a catchment. Measurements of those environmental tracers in discharge can be used to infer transit time distributions (TTDs) and mean transit times (MTTs) on the catchment scale. These inferred TTDs and MTTs might in turn enable a deeper understanding of hydrological processes which cannot be assessed by discharge measurements alone.

Transit time estimations based on lumped modelling approaches have been carried out in various studies, reviewed by McGuire and McDonnell (2006), and subsequent studies like Soulsby and Tetzlaff (2008), Tetzlaff et al. (2009b), Hrachowitz et al. (2010), Roa-García and Weiler (2010), Lyon et al. (2010), Soulsby et al. (2011), Heidbüchel et al. (2012), and Capell et al. (2012).

McGuire and McDonnell (2006) pointed out that the widespread lumped convolution model approach was originally developed for groundwater systems (Małozzewski and Zuber, 1982) and assumes a hydrological steady state system (Małozzewski et al., 1983) and a determinable representative input. For catchments these assumptions are often violated. Consequently, more recent studies abandoned the steady state assumption in favour of convolution model approaches with time variant TTDs (Hrachowitz et al., 2010; Heidbüchel et al., 2012) or even more flexible explicit modelling approaches (Hrachowitz et al., 2013). While these approaches are more suited to capture the mostly short-term time variable behaviour of transit times in catchments, they come at a higher computational cost and require more extensive input data time series than usually available. In addition, other assumptions are required to apply these time variant approaches. Even though the application of time invariant transfer functions might lead to a less satisfactory fit to observed tracer signals, their indisputable advantage lies in their comparatively simple implementation and less extensive input data requirements (Mueller et al., 2013).

## HESSD

11, 6753–6803, 2014

### Convolution models revisited

S. Seeger and M. Weiler

Title Page

Abstract

Introduction

Conclusions

References

Tables

Figures

⏪

⏩

◀

▶

Back

Close

Full Screen / Esc

Printer-friendly Version

Interactive Discussion



**Convolution models  
revisited**

S. Seeger and M. Weiler

[Title Page](#)[Abstract](#)[Introduction](#)[Conclusions](#)[References](#)[Tables](#)[Figures](#)[⏪](#)[⏩](#)[◀](#)[▶](#)[Back](#)[Close](#)[Full Screen / Esc](#)[Printer-friendly Version](#)[Interactive Discussion](#)

Several studies were dedicated to the investigation of the relationship between catchment topography and mean transit times. McGuire et al. (2005) as well as Tetzlaff et al. (2009b) found a strong correlation between MTTs and the ratio of the median overland flow distance to median flow path gradient ( $L/G$ ) for nested catchment studies in the Western Cascades of Oregon and the Scottish Cairngorm mountains, respectively. Hrachowitz et al. (2009), on the other hand, found no significant correlation between MTTs and  $L/G$ . They identified the catchments' proportions of responsive soils and their drainage densities as best predictors of MTTs. Soulsby and Tetzlaff (2008) and Capell et al. (2012) also found good correlations between MTTs and the proportions of responsive soils. Probably due to the small sample size of four catchments, Mueller et al. (2013) found no significant correlation between MTTs and any topographic index, but the highest correlation coefficient of 0.62 was obtained for the drainage density of base flow streams. They did not test for a correlation to  $L/G$ . In a comparative study Tetzlaff et al. (2009a) used the damping ratio of standard deviations of  $\delta^{18}\text{O}$  in precipitation and discharge as transit time proxy (TTP) instead of MTTs to investigate catchments of various geomorphic regions across the Northern Hemisphere and also found a strong correlation to  $L/G$ .

The objective of this study was to determine MTTs of 24 catchments in Switzerland and to assess their relationship to topographical indices, with the final aim of finding a topography driven regionalisation method. Due to limited input data availability and the comparatively high number of catchments, we chose the basic lumped convolution model approach and assumed time invariant transfer functions. The influence of water retention and release by snow storage in alpine catchments necessitated the development of a snow module, which accounts for the isotopic composition of snow storage and melt water. Another focus of this study was laid on a comparison of the MTT estimates from different transfer functions and the assessment of the suitability of different transfer function types.

## 2 Data

### 2.1 Study area

This study focused on 24 catchments distributed across the Swiss Plateau and the Swiss Alps (see Fig. 1), selected based on the following criteria: least possible human influence, glaciers covering less than 5% of the catchment area, possibility for collecting isotope samples and data availability. The catchment area, mean elevation and average annual precipitation is listed for all catchments in Table 1. The mean catchment elevations are between 472 m and 2369 m a.s.l. and their areas range from 0.7 to 351 km<sup>2</sup>. The dominating landcovers within these catchments are elevation dependent, with agricultural areas dominating at lower elevations (< 800 m), grasslands, pastures and forests at mid altitudes (800–1400 m) and grasslands or sparsely vegetated areas at higher elevations > 1700 m. Minor fractions of the catchments *Schaechen* and *Dischmabach* (2 and 5%, respectively) are glaciated and around 10% of the catchments *Biber* and *Aabach* are covered with permanent wetlands or open water.

Mean annual catchment precipitations range from 1012 to 2600 mm and their seasonal distributions are slightly skewed towards the summer half-year with 54 to 61% of annual precipitation. Primarily elevation dependent temperature differences cause a range of discharge regimes from pluvial for the colline and submontane catchments to nival for the more alpine catchments. Different underlying geologies, from crystalline and limestone in the Alps to flysch and molasse in the Swiss Plateau, in connection with varying topographical conditions led to a variety of soils and further differences in discharge behavior among the catchments.

### 2.2 Discharge data and meteorological data

The Swiss Federal Office for the Environment (FOEN) provided the daily discharge data for most of the catchments. Discharge data for the catchments *Luempenenbach*,

# HESSD

11, 6753–6803, 2014

## Convolution models revisited

S. Seeger and M. Weiler

Title Page

Abstract

Introduction

Conclusions

References

Tables

Figures

⏪

⏩

◀

▶

Back

Close

Full Screen / Esc

Printer-friendly Version

Interactive Discussion



*Erlenbach* and *Vogelbach* were obtained from the Swiss Federal Institute for Forest, Snow and Landscape Research (WSL). Additional discharge data for the catchments *Roethebach* and *Emme* were provided by the Amt für Abwasser und Umwelt (AWA) of the Swiss Canton Berne.

The climate data, like average catchment precipitation, temperature, relative air humidity, wind speed and global radiation for 100 m elevation bands in each catchment based on interpolated site data from the national meteorological service of Switzerland (MeteoSwiss) were provided by the PREVAH working group (Viviroli et al., 2009a, b).

### 2.3 Discharge isotope data

All isotopic compositions in this study are expressed in the  $\delta$  notation according to the VSMOV-standard. Water samples at the catchment outlets were taken fortnightly from mid 2010 to end 2012. The 100 mL samples were analyzed for stable water isotopes with a PICARRO cavity ringdown spectrometer at the Chair for Hydrology at the University of Freiburg, Germany. According to the manufacturer's specifications the measurement accuracy for  $\delta^{18}\text{O}$  and  $\delta^2\text{H}$  is 0.16 and 0.6‰, respectively. Additional discharge isotope data before 2010 for the catchment *Rietholzbach Mosnang* and its subcatchment *Oberer Rietholzbach* was received from the Institute for Atmospheric and Climate Science (IAC) of the Swiss Federal Institute of Technology (ETH), Zurich. Therefore, the available discharge isotope time series for those two catchments extent further into the past, though no discharge isotope samples for the subcatchment *Oberer Rietholzbach* have been taken after February 2010.

As  $\delta^{18}\text{O}$  and  $\delta^2\text{H}$  data records convey the same information and the availability of  $\delta^{18}\text{O}$  values was better than for  $\delta^2\text{H}$ , this study concentrated on  $\delta^{18}\text{O}$  values, occasionally referring to them as *isotopic composition*.

**HESSD**

11, 6753–6803, 2014

## Convolution models revisited

S. Seeger and M. Weiler

Title Page

Abstract

Introduction

Conclusions

References

Tables

Figures

⏪

⏩

⏴

⏵

Back

Close

Full Screen / Esc

Printer-friendly Version

Interactive Discussion



## 2.4 Precipitation isotope data

The National Network for the Observation of Isotopes in the Water Cycle (NAQUA-ISOT) of the Federal Office for the Environment (FOEN) of Switzerland measures stable water isotopes ( $\delta^{18}\text{O}$  and  $\delta^2\text{H}$ ) in the precipitation at monthly intervals at 13 sites. Supplemental data were taken from 5 sites of the Austrian Network of Isotopes in Precipitation (ANIP) and 5 sites of the Global Network of Isotopes in Precipitation (GNIP). Figure 1 shows the positions of these sites. The highest data availability is given for the period between July 1992 and October 2011, where at least for eleven sites monthly values were available.

## 3 Methods

### 3.1 Derivation of topographic indices

In order to derive topography based indices for the 24 catchments, a topographic terrain analysis based on a digital elevation model (DEM) with a resolution of 25 m was carried out with the free open source software SAGA-GIS (Conrad et al., 2013). In a first step, the SAGA module “Channel Network” was used to derive the channel network for each catchment. The required initiation threshold was adapted manually for each catchment to achieve the best agreement between the computed channel networks and the channel networks observed in maps and areal imagery, in our case from Google Maps WMS (Web Map Service) layers.

The SAGA module “Overland Flow Distance to Channel network” was used to calculate the flow path lengths  $L$  as well as their respective horizontal and vertical components ( $L_h$  and  $L_v$ ) for the 24 catchments. Furthermore, the flow gradient  $G$  was computed as the ratio  $L_v/L_h$ . These values were aggregated for each catchment by computing each catchment’s median values. Eventually, the ratio  $L/G$  was computed for each of the study catchments. Additionally, the topographic wetness indices (TWI)

HESSD

11, 6753–6803, 2014

## Convolution models revisited

S. Seeger and M. Weiler

Title Page

Abstract

Introduction

Conclusions

References

Tables

Figures

◀

▶

◀

▶

Back

Close

Full Screen / Esc

Printer-friendly Version

Interactive Discussion



were computed with the module “Topographic Wetness Index” (Böhner and Selige, 2006) and again aggregated by computing their median values for each catchment. Drainage densities (DD) were computed as the ratio of raster cells containing a part of the channel network to the total number of the catchments’ raster cells.

### 3.2 Spatial interpolation of precipitation isotope data

The isotopic composition of precipitation is required as input for modelling transit time distributions. Since it was not directly measured within the catchments, the following procedure to interpolate the available site data was applied:

I Based on the  $\delta^{18}\text{O}$  values of the three measurement sites *Meiringen*, *Guttannen* and *Grimsel*, which lie along an elevation transect in the Bernese Alps between 632 and 1950 m a.s.l. (see the bold red line in the map in Fig. 1), average height gradients  $\bar{g}$  for each month were computed. It was assumed that these gradients are representative for the whole study area.

II Monthly and average monthly  $\delta^{18}\text{O}$  values corrected to the sea level elevation ( $i_s$  and  $\bar{i}_s$ ) were computed for every measurement site  $s$  as follows:

$$i_s = I_s + h_s \cdot \bar{g} \quad (1)$$

$$\bar{i}_s = \bar{I}_s + h_s \cdot \bar{g} \quad (2)$$

where  $I_s$  is the isotopic composition for measurement site  $s$  with the site elevation  $h_s$  for a certain month and year, while  $\bar{I}_s$  is the same, but averaged over all years for each month.

III The average monthly elevation corrected  $\delta^{18}\text{O}$  values  $\bar{i}_s$  for all measurement sites were spatially interpolated using kriging (Delhomme, 1978), implemented in the *gstat*-package (Pebesma, 2004) for  $R$ . This resulted in continuous maps of average monthly sea level  $\delta^{18}\text{O}$  values for every point  $p$  within the study region for each month of the year.

IV To derive the  $\delta^{18}\text{O}$  value for a certain location  $p$  at a specific year and month,  $l_p$ , the following equations were used:

$$d_{s^*} = i_{s^*} - \overline{i_{s^*}} \quad (3)$$

$$i_p = \overline{i_p} - d_{s^*} \quad (4)$$

$$l_p = i_p - h_p \cdot \overline{g} \quad (5)$$

First, the measurement site closest to the location  $p$  was chosen, denoted as  $s^*$ . In Eq. (3), the deviation  $d_{s^*}$  for a specific month's  $\delta^{18}\text{O}$  value to its according average monthly value was computed for the measurement site  $s^*$ . By subtracting this deviation from the average monthly sea level  $\delta^{18}\text{O}$  value at the location  $p$ , obtained from the interpolation in step III, the specific month's sea level  $\delta^{18}\text{O}$  value at point  $p$  was estimated in Eq. (4). Finally  $h_p$ , the elevation of the point of interest, was taken into account to obtain the actual  $\delta^{18}\text{O}$  value  $l_p$  at the location  $p$  in Eq. (5). Since most measurement sites have data gaps during the investigation period,  $s^*$  for the same  $p$  can refer to different sites for different time steps.

### 3.3 Transit time proxy

To complement the lumped convolution modelling, we adapted the inverse transit time proxy (ITTP) approach described by Tetzlaff et al. (2009a), similar to an approach used by DeWalle and Edwards (1997):

$$\text{ITTP} = \frac{\sigma_{C_Q}}{\sigma_{C_p}} \quad (6)$$

According to Eq. (6), the ITTP is computed as the ratio of the standard deviations of  $\delta^{18}\text{O}$  values in discharge ( $\sigma_{C_Q}$ ) and precipitation ( $\sigma_{C_p}$ ). The ITTP reflects the precipitation input signal's damping in the discharge and showed an inverse

Title Page

Abstract

Introduction

Conclusions

References

Tables

Figures

⏪

⏩

◀

▶

Back

Close

Full Screen / Esc

Printer-friendly Version

Interactive Discussion



proportionality to MTT estimates. For clarity's sake we preferred to use the inverted ITTP – the transit time proxy TTP. Instead of long time series of climatic input data and stream discharge measurements, this approach only requires time series of the isotopic compositions of precipitation and stream water (Tetzlaff et al., 2009a).

### 5 3.4 Model framework

The model framework in this study is based on the TRANSEP-framework (Weiler, 2003), without the distinction of event and pre-event water and extended by a snow module to encounter the specific conditions in alpine catchments. Figure 2 provides an overview on the model structure and the data flow.

#### 10 3.4.1 Distributed snow modelling

Since many of the selected catchments are heavily influenced by snow accumulation and snow melt processes, the implementation of a snow model was crucial. Due to a lack of suitable snow data for the calibration of a simple parameterized snow model and the availability of the appropriate climatic input data, a point-energy-balance based approach was chosen. This study uses a modified implementation of *ESCIMO* (Energy balance Snow Cover Integrated *MO*del by Strasser and Marke, 2010), based on *ESCIMO.spread* and requires hourly input values for air temperature, precipitation amount, wind speed, relative humidity as well as for incoming short- and longwave radiation. To account for the available input data, the following modifications were made:

- change of time step length from hourly to daily (significant snowfall rate of  $0.5 \text{ mm h}^{-1}$  to reset the albedo to its maximum value was adapted to  $2 \text{ mm d}^{-1}$ )
- calculation of incoming longwave radiation with available input data and an empirical relationship given in Sicart and Hock (2010)

## Convolution models revisited

S. Seeger and M. Weiler

Title Page

Abstract

Introduction

Conclusions

References

Tables

Figures

⏪

⏩

◀

▶

Back

Close

Full Screen / Esc

Printer-friendly Version

Interactive Discussion



## Convolution models revisited

S. Seeger and M. Weiler

Title Page

Abstract

Introduction

Conclusions

References

Tables

Figures

⏪

⏩

◀

▶

Back

Close

Full Screen / Esc

Printer-friendly Version

Interactive Discussion



Like the original *ESCIMO*, this modified version predicts melt water amounts and sublimation. Under the simplifying assumptions of complete mixing in the snow pack and negligible influence of fractionation processes, further minor modifications like the computation of weighted averages of snow pack and new snow enabled the prediction of average isotopic compositions of the snow pack and hence the melt water. Due to the distinct elevation dependence of snow accumulation and melt processes, it was decided to run the snow module for different elevation bands in each catchment. Melt water amounts (including precipitation not retained in the snow pack), sublimation from the snow pack and the isotopic composition of the melt water for all elevation levels of a catchment were then aggregated to calculate the average catchment wide liquid input for the next modelling steps.

### 3.4.2 Lumped discharge and isotope modelling

Discharge and its isotopic compositions were simulated with two similar lumped convolution models. Both of these models require effective precipitation as their input. The effective precipitation was obtained from a rainfall-loss module. While the proposed modelling framework is not bound to any particular method for computing the effective precipitation, we used the approach described by Jakeman and Hornberger (1993), which computes effective precipitation based on a storage index that underlies a decay rate depending on temperature. For further details see Jakeman and Hornberger (1993) or Weiler (2003).

Discharge  $Q$  for a certain time step  $t$  is described by a convolution of the hydraulic transfer function  $h(\tau)$  with all preceding effective precipitation values  $p_{\text{eff}}$  (Weiler, 2003):

$$Q(t) = \int_0^t h(\tau) p_{\text{eff}}(t - \tau) d\tau \quad (7)$$

The tracer concentration in discharge  $C(t)$  is computed in a similar way. Instead of the effective precipitation, the mass weighted isotopic composition of the precipitation,

$C_P(t)$ , is convoluted by the tracer transfer function, or transit time distribution (TTD),  $g(\tau)$  (Stewart and McDonnell, 1991; Weiler, 2003; Hrachowitz et al., 2010):

$$C(t) = \frac{\int_0^t g(\tau) \rho_{\text{eff}}(t - \tau) C_P(t - \tau) dt}{\int_0^t g(\tau) \rho_{\text{eff}}(t - \tau) d\tau} \quad (8)$$

### 3.4.3 Transfer functions

Table 2 shows all transfer functions used in this study: the widely used exponential model (EM), described by Małozzewski and Zuber (1982); the more flexible gamma distribution model (GM), described by Kirchner et al. (2000) and the two parallel linear reservoir (TPLR) model (Weiler, 2003). Both, the GM as well as the TPLR, have special cases in which they are equal to the EM.

The discharge convolution module was mainly needed as an auxiliary mean to constrain the parameters of the rainfall-loss module. As initial testing revealed, the TPLR was clearly outperforming the GM and the EM as hydraulic transfer function and was therefore a priori selected as the sole hydraulic transfer function  $h(\tau)$  of this study.

Regardless whether previous transit time studies mentioned different tracer transfer functions or not, for catchment comparisons most of them focused on one of them: McGuire (2005) and Mueller et al. (2013) chose the EM; Hrachowitz et al. (2010), Soulsby et al. (2011), Birkel et al. (2012) and Heidbüchel et al. (2012) chose the GM while Roa-García and Weiler (2010) selected the TPLR. An exception is a nested catchment study by Capell et al. (2012), who fitted GM as well as TPLR to eight catchments and considered both model types throughout the analysis of the results. When we implemented the mathematically defined transfer functions into the model framework, the issue of transfer function normalisation arose. The mathematical considerations of this are explained in Appendix A. As normalisation might have a great impact on the shape of a transfer function and the mean transit time, normalised and not normalised variants of the same transfer function were distinguished in this study, denoting the normalised variant with an asterisk, i.e. the normalised variant of the

## Convolution models revisited

S. Seeger and M. Weiler

Title Page

Abstract

Introduction

Conclusions

References

Tables

Figures

⏪

⏩

◀

▶

Back

Close

Full Screen / Esc

Printer-friendly Version

Interactive Discussion



TPLR was called TPLR\*. In this study we refrained from an a priori selection of the tracer transfer function type and chose to optimise our models for each of the three transfer functions and their normalised and non-normalized variants.

### 3.5 Model optimisation and uncertainty

5 Due to the large amount of optimisations (six models at seven to nine parameters for 24 catchments) Monte Carlo sampling was deemed impracticable for this study. Instead, a multi objective optimisation approach using the NSGA-II algorithm after Deb et al. (2002), implemented in the R-package *mco* by Trautmann et al. (2013), was chosen to obtain pareto-optimal parameter sets based on the agreement between simulated and  
10 observed values for discharge and isotope concentrations in discharge.

Three objective functions were applied to evaluate the model:  $KGE'(Q)$  and  $KGE'(\log(Q))$  were selected to compare the simulated discharge values against the observed values and  $KGE^-(C)$  was used to compare the simulated isotopic composition of the discharge against the  $\delta^{18}O$  values observed in the discharge.

15  $KGE'$  is the modified Kling-Gupta Efficiency after Gupta et al. (2009) and Kling et al. (2012), which consists of a combination of the correlation coefficient, the ratio of standard deviations and the ratio of mean values. For the evaluation of simulated isotope concentrations, possible biases caused by the spatial interpolation of sparse input data had to be ignored. Therefore a reduced variant of the  $KGE'$ , called  $KGE^-$ ,  
20 that only takes into account the correlation coefficient and the ratio of standard deviations was applied.

The multi-objective NSGA-II optimisation algorithm was run for each of the 24 catchments and each of the six isotope transfer function models with a population size of 1500 and 20 generations. In case the first run of the algorithm did not produce  
25 at least 300 pareto-optimal parameter sets, the found solutions were remembered and the algorithm was repeated as often as needed.

Not all of the pareto-optimal parameter sets lead to reasonable solutions, as at a certain point minimal improvements in respect to the value of one objective function

## Convolution models revisited

S. Seeger and M. Weiler

Title Page

Abstract

Introduction

Conclusions

References

Tables

Figures

⏪

⏩

⏴

⏵

Back

Close

Full Screen / Esc

Printer-friendly Version

Interactive Discussion



lead to substantial deterioration of the values of the other objective functions. Similarly to combining three single objective functions into one for the Kling-Gupta Efficiency (Gupta et al., 2009), we used  $D_0$ , the euclidean distance to the ideal point (in our case zero), to evaluate the overall goodness of a parameter set:

$$D_0 = \sqrt{(1 - E(Q))^2 + (1 - E(\log(Q)))^2 + (1 - E_r(C))^2} \quad (9)$$

In Eq. (9),  $E$  stands for  $KGE'$  and  $E_r$  stands for the previously explained reduced variant,  $KGE^-$ .

The results of the iterative meta-heuristic NSGA-II algorithm are not suited to be used within the established Generalized Likelihood Uncertainty Estimation (Beven and Binley, 1992) method, which would require big numbers of parameter sets obtained by random sampling over the whole parameter value ranges. Therefore another approach to estimate model uncertainty was utilised. All parameter sets with a  $D_0$  smaller than the 10% quantile of all parameter sets'  $D_0$  were considered acceptable. Parameter- and prediction uncertainties were then given by the ranges encompassed by all acceptable parameter sets and their respective simulation results. Most comparisons and analysis presented in this study refer to the median values of all acceptable solutions.

### 3.6 Transit time distribution comparison

To compare the characteristics of the six model types' TTDs across all catchments, we started by identifying the best model type for each catchment, i.e. the model type which reached the highest objective function value for its simulated isotopic compositions in discharge. This set of the best models served as a reference against which the six model types were compared. We compared the models under the two aspects: time after which a certain cumulated transfer function (TF) value is reached and the cumulated TF value reached after a certain time. Coefficients of determination as well

## Convolution models revisited

S. Seeger and M. Weiler

Title Page

Abstract

Introduction

Conclusions

References

Tables

Figures

⏪

⏩

⏴

⏵

Back

Close

Full Screen / Esc

Printer-friendly Version

Interactive Discussion



as the mean ratio of the reference values and the respective values of a specific model were computed.

## 4 Results

### 4.1 Spatial interpolation of isotopes in precipitation

5 Monthly elevation gradients of  $\delta^{18}\text{O}$ , averaged over the time period from mid 1992 to the end of 2011, computed along the three *NAQUA-ISOT* sites *Meiringen*, *Gutannen* and *Grimsel* reached values between  $-0.10\text{‰}$  per 100 m for January and  $-0.25\text{‰}$  per 100 m for September, with an overall mean value of  $-0.21\text{‰}$  per 100 m. This is in good agreement with the values reported for the same region by Siegenthaler and Oeschger (1980) and Mueller et al. (2013). The interpolated average monthly  $\delta^{18}\text{O}$  values at sea level shown in Fig. 3 reveal a seasonal pattern, where  $\delta^{18}\text{O}$  values at sea level from May to September are higher and far more homogeneous than from October to April. Biggest differences occur from December to March, where  $\delta^{18}\text{O}$  values at sea level clearly decline in a south-eastern direction. A qualitative validation of the interpolation based predictions can be found in Appendix B.

### 4.2 Model optimisation and parameter identifiability

For some catchments, the required number of 300 pareto-optimal solutions was exceeded after the first run and it could easily be increased to 1000, for other catchments the required number of 300 pareto-optimal solutions demanded many repetitions of the optimisation algorithm. Consequently, the number of acceptable solutions and the quality of the pareto-fronts varied between the catchments and the models and parameter ranges are based on 30–100 parameter sets. The parameters of the rainfall loss module after Jakeman and Hornberger (1993) could hardly be identified – in many cases two of the three parameters spanned over wide ranges of the whole possible values. For the TPLR hydraulic transfer model,  $\tau_f$  and  $\phi$  could

## Convolution models revisited

S. Seeger and M. Weiler

Title Page

Abstract

Introduction

Conclusions

References

Tables

Figures

⏪

⏩

◀

▶

Back

Close

Full Screen / Esc

Printer-friendly Version

Interactive Discussion



## Convolution models revisited

S. Seeger and M. Weiler

Title Page

Abstract

Introduction

Conclusions

References

Tables

Figures

⏪

⏩

◀

▶

Back

Close

Full Screen / Esc

Printer-friendly Version

Interactive Discussion



be identified quite well, while the values for  $\tau_s$  often covered large parts of the possible value range. Unsurprisingly, the EM with only one parameter showed the best parameter identifiability amongst all transfer functions (from now on TFs). Even when the parameters of the rainfall-loss models proved to be unidentifiable, in most cases  $\tau_m$  of the EM could be constrained to rather narrow ranges. Solely for the catchments *Aabach* and *Mentue*  $\tau_m$  varied by orders of magnitude. The two parameters of the GM generally proved to be identifiable, even though in some cases they exhibited a notable range. As expectable, parameter identifiability for the three parameter TPLR transfer function was the lowest. Similarly to the TPLR hydraulic transfer model,  $\tau_f$  and  $\phi$  tended to be more identifiable than  $\tau_s$ .

### 4.3 Rainfall-discharge model

Independently from the six different isotope TF models, the rainfall-runoff component of the model performed equally satisfactory for most of the studied catchments, reaching  $KGE'$  and  $KGE'_{\log}$  values between 0.7 and 0.9 for most of them (see Fig. 4). Notable exceptions are *Riale di Calneggia*, whose  $KGE'$  value of 0.6 is still acceptable but below the values of the other catchments, *Erlenbach* and *Vogelbach* with  $KGE'_{\log}$  values around 0.5 and *Oberer Rietholzbach* with  $KGE'$  values below 0.3 and  $KGE'_{\log}$  values around 0.6. Not only the values of the discharge based objective functions, but also the optimised parameter values for the rainfall-runoff component of the model turned out to have the same values, no matter which tracer transfer function was part of the multi-objective optimisation. Obviously, the application of the snow module was essential for good performance of the rainfall-runoff model in particular for catchments at higher elevations.

## 4.4 Isotope composition model

### 4.4.1 Performance

Objective function values for the prediction of isotopic compositions in discharge for the six different TF models are listed in the lower part of Fig. 4, while the left column of Fig. 5 shows the simulated and observed  $\delta^{18}\text{O}$  values for five selected catchments. The differences represented in the objective function values between normalised and not normalised variants for one of the three basic transfer function types were negligible for most of the catchments (Fig. 4). For the four catchments *Guerbe*, *Sitter* (see third column of Fig. 5), *Riale di Calneggia* and *Schaechen*, all models performed similarly well. Comparison of simulated and observed  $\delta^{18}\text{O}$  values in discharge as well as the objective function values suggest a less satisfactory performance of the EM transfer function for the other catchments. Beyond that, it is not possible to announce an overall superior TF type: The three parameter TPLR models often reached the highest objective function values, but for some catchments the two parameter GM reached higher values. For many catchments the GM and TPLR performed very similarly, even though the simulated  $\delta^{18}\text{O}$  values in discharge were not the same for the two model types, as the GM tended to produce more short term variability than TPLR.

### 4.4.2 Prediction bias

Regardless of the applied model types, all predicted  $\delta^{18}\text{O}$  time series in discharge were biased in one or the other direction (for some examples see the result of the bias calculation shown in the middle column of Fig. 5). A negative prediction bias means that the predicted  $\delta^{18}\text{O}$  values in discharge were lower than the respective observed values. These biases were not taken into account for the computation of the respective objective function values. For most catchments, the bias for all six TTDs varied within a range of 0.5‰  $\delta^{18}\text{O}$ . Larger differences between different models' bias values were observed for the catchments at higher elevation, with a maximum

HESSD

11, 6753–6803, 2014

## Convolution models revisited

S. Seeger and M. Weiler

Title Page

Abstract

Introduction

Conclusions

References

Tables

Figures

⏪

⏩

◀

▶

Back

Close

Full Screen / Esc

Printer-friendly Version

Interactive Discussion



bias for the catchment *Dischmabach*, where the biases of the not normalised TPLR model were around  $-0.2\text{‰ } \delta^{18}\text{O}$ , while the biases of the other models were distinctly higher and reached  $2\text{‰ } \delta^{18}\text{O}$ . An elevation dependent grouping was observed: the 16 catchments at mean elevations up to 1300 m.a.s.l. showed negative biases around  $-0.7\text{‰}$  (ranging from  $-0.1$  to  $-1.3\text{‰}$ ), while seven catchments with higher mean elevations showed more positive biases between  $-0.2$  and  $2\text{‰}$ . The transition between those two groups is not gradually but abrupt. Being the only catchment south of the Alps, *Riale di Calneggia* with a mean elevation of nearly 2000 m.a.sl. showed high negative biases around  $-2\text{‰}$ .

#### 4.4.3 Intercomparison of transfer functions

Despite the quite similar performance of the different TTDs in the catchments independent of taking normalisation of the transfer function into account, a clear differences of the TTD shapes and the resulting MTTs for TPLR and GM was observed (Fig. 6). For TTDs with long tailings, the normalised and not normalised variants clearly diverge for longer transit times (see right column of Fig. 6).

This effect also alters the resulting MTTs as illustrated in Fig. 7. As the EM generally lacks long tailings, normalisation did not affect the results and the MTTs for the normalised and not-normalised variants were identical. For the eleven catchments with the shortest MTTs, normalisation did not affect the GM, i.e. both variants were similar and resulted in similar MTTs. But for catchments with longer MTTs normalisation resulted in the described divergence of the tailings of the TTDs and hence in a significant increase in the resulting MTTs (up to 4 times higher). An even stronger effect of the normalisation was observed for the TPLR models, where normalisation also tended to distort the TTDs of catchments with small MTTs (see the blue highlighted lines in the top right section of Fig. 6).

The MTTs for all TFs agreed only for two catchments: *Schaechen* (MTT of 1.2 years) and *Sitter* (MTTs between 0.7 and 0.9 years). For the other catchments, the MTT estimates of the different model types occasionally varied by orders of magnitude. One

Title Page

Abstract

Introduction

Conclusions

References

Tables

Figures

⏪

⏩

◀

▶

Back

Close

Full Screen / Esc

Printer-friendly Version

Interactive Discussion



## Convolution models revisited

S. Seeger and M. Weiler

Title Page

Abstract

Introduction

Conclusions

References

Tables

Figures

◀

▶

◀

▶

Back

Close

Full Screen / Esc

Printer-friendly Version

Interactive Discussion



example is the catchment *Langeten* (see top of Fig. 5): while both EM variants result in a MTT of 2.3 years, the not-normalised variants of TPLR and GM result in a MTT of 67.2 and 29 years, respectively, whereas their normalised variants show a MTTs of 8.4, and 6.1 years, respectively. Despite the distinctly different MTT estimates, nearly identical objective function values were reached by the two variants of the TPLR.

The ranking of the calculated MTTs for the different models appeared more or less consistent. Spearman's rank correlation coefficients ( $\rho$ ) and Pearson correlation coefficients ( $r$ ) and their respective  $p$  values were computed to assess the relationships between the MTTs estimated with the six different model types as well as the transit time proxy (TTP) (Fig. 8). Correlations between the EM and TPLR models proved to be the lowest (correlation coefficients between 0.30 and 0.49). For all other combinations the correlations were clearly significant with  $p$  values less than 0.005. The TTP significantly correlated with all models' MTT estimates and reached rank correlation coefficients between 0.61 (for MTTs based on normalised TPLR) and 0.92 (for MTTs based on normalised GM).

The comparison of the cumulated TTDs of the six model types (examples for five selected catchments in the right column of Fig. 5) showed that the differences between the model types were greatest towards the longer transit times. For some catchments there were also notable differences between different model types towards the shortest transit times. Instead of discussing the cumulated TTD curves for all 24 catchments of each of the six models individually, Fig. 9 shows the coefficients of determination and the mean cumulated TTD value ratios between a specific model type and the respective best model for each catchment as described in Sect. 3.6. Figure 9 shows that for the GM and TPLR the coefficient of determination as well as the mean value ratios reached values close to one around a time of three months. This means that after an elapsed time of around three months each variant of these two model types led to very similar cumulated TTD values, which were also close to the values of the overall best performing model of all the six applied models. For longer and shorter times, the coefficients of determination declined and the mean value ratios started to diverge from

one, which means that the cumulated TTDs of the models were generally less similar and further apart from the respective best model's TTD.

#### 4.4.4 Relation between topographic indices and mean transit times

Without discussing all topographic indices (see Table 3) in detail, it seems noteworthy to point out that TWI,  $G$ ,  $L/G$  and were significantly ( $p < 0.05$ ) correlated to each other and to the mean catchment elevation. The higher the catchments, the bigger were the gradients  $G$ , the smaller the ratios  $L/G$  and the smaller the topographic wetness indices. Apparently all three indices are correlated to the steepness of the catchments. The catchments *Aach*, *Aabach* and (to a lesser degree) *Mentue* proved to be much flatter than the remaining catchments and to avoid a distortion of the results caused by a leverage effect, correlations between MTTs and topographic indices were computed for all and excluding these three catchments.

Table 4 shows the correlation coefficients  $r$  and  $\rho$  between the MTTs based on different TF models (and the TTP) and the topographic indices as well as catchment areas, mean elevations and mean annual precipitation sums. When all catchments were included (first section of Table 4), there were significant Pearson correlations between the MTTs of the not normalised GM and the mean catchment elevation and the median flowpath gradient  $G$ , as well as between the MTTs of the normalised GM and the drainage density  $DD$ . Except for the two EM variants, there were further significant rank correlations between MTTs (and the TTP) and the ratio  $L/G$  and between the both TPLR variants' MTTs (and the TTP) and  $DD$ . When the same correlations were computed without the aforementioned three flattest catchments, the picture changed a bit (second section of Table 4). Most notably, except for the normalised TPLR model, the correlations between MTTs (and the TTP) and the ratio  $L/G$  were higher and nearly all but one were significant.

However, the strongest correlations were found between MTTs (and TTPs) and the mean annual precipitation sums of the catchments. This is not surprising, as higher inputs into the same storage system consequently should lead to higher turnover

## Convolution models revisited

S. Seeger and M. Weiler

Title Page

Abstract

Introduction

Conclusions

References

Tables

Figures

⏪

⏩

◀

▶

Back

Close

Full Screen / Esc

Printer-friendly Version

Interactive Discussion





and the positive biases for the higher situated catchments can, for the most part, be explained by systematic errors of other model components (see next section), the interpolation method can be considered suitable for this application. More sophisticated interpolation procedures, taking other influence factors such as air temperatures, precipitation amounts, windward-leeward effects and dominant weather situations into account, are conceivable, but to the authors' knowledge up to the present there is no such interpolation method for the given temporal and spatial scales available and its development clearly exceeded the scope of this study.

### 5.3 Prediction bias of streamwater stable isotopes

The convolution model could adequately reproduce the seasonal variations of the isotope concentrations in streamwater, however all predictions exhibited a bias. For most of the catchments, the biases were independent from the applied transfer function, indicating that the systematic bias was not caused by the choice of transfer functions. Upon closer inspection, three possible reasons for this bias have to be considered:

First, there could be a bias in the precipitation isotopes, caused by incorrect assumptions made during the interpolation of the sparse measurement site data. The resulting biases could be positive or negative and are more likely to occur in regions where the surrounding measurement sites are further apart and the catchment elevations exceed the elevations of the measurement sites.

Another error source for the input isotope concentration of alpine catchments could be assumptions made for the snow module. Particularly the assumption of isotopical homogeneous melt from the snow pack without significant enrichment is debatable as Taylor et al. (2001) as well as Unnikrishna et al. (2002) observed a range of melt water  $\delta^{18}\text{O}$  values of up to 3‰ around the snow pack's mean isotopic composition. Furthermore, Taylor et al. (2001) measured an overall  $\delta^{18}\text{O}$  enrichment of around 0.3‰ for the entire melt water amount. While this could explain deviations during the ablation period, it is not sufficient to explain the observed overall bias values of

## Convolution models revisited

S. Seeger and M. Weiler

Title Page

Abstract

Introduction

Conclusions

References

Tables

Figures

⏪

⏩

◀

▶

Back

Close

Full Screen / Esc

Printer-friendly Version

Interactive Discussion



around 1‰ for the alpine catchments, unless the enrichment effect observed in the two aforementioned studies, both of them conducted in the Californian Sierra Nevada, is more pronounced for our study region.

The third possible cause of the prediction biases is inherent to the model, more precisely its rainfall-loss module. Since there is no representation of a soil storage, where winter- and summer precipitation can mix to a certain extent, the simulated evapotranspiration, occurring predominantly during summer, consists almost entirely of the isotopically heavier summer precipitation. On the other hand, nearly all of the isotopically lighter winter precipitation is routed to discharge. While it is likely, that the largest part of the yearly evapotranspiration stems from summer precipitation and that a larger fraction of winter precipitation contributes to discharge, it can be assumed that the missing model representation of a mixing soil storage necessarily leads to a prediction bias towards lighter discharge isotope concentrations. This kind of bias might be prevalent at the non-alpine catchments, where all predictions have a slightly negative bias between 0 and  $-1\text{‰ } \delta^{18}\text{O}$ , while no such bias can be recognised when the interpolated precipitation isotope concentrations are compared to the validation site data (see Appendix B) in the same region.

#### 5.4 Temporal scope of the modelling approach

The coarse temporal resolution of the isotopic input data is not suited to evaluate the short-term behaviour of the TTDs. Consequently these differences are unaccounted for by the objective function since only fortnightly data in streamflow was available. At the same time, the increased dampening of the seasonal variation of the  $\delta^{18}\text{O}$  signal in precipitation after a few years inevitably leads to a point, where the measurement uncertainties and faster components of the TTD wholly conceal the part of the signal which is caused by the long tailing of the TTD, which in turn also excludes the slowest fraction of a TTD from an objective evaluation using stable water isotopes. In fact, the inter-model comparison in Fig. 9 suggests that, at least for the available fortnightly stream sample data in combination with the monthly aggregated precipitation isotope

## Convolution models revisited

S. Seeger and M. Weiler

Title Page

Abstract

Introduction

Conclusions

References

Tables

Figures

⏪

⏩

◀

▶

Back

Close

Full Screen / Esc

Printer-friendly Version

Interactive Discussion



## Convolution models revisited

S. Seeger and M. Weiler

Title Page

Abstract

Introduction

Conclusions

References

Tables

Figures

⏪

⏩

◀

▶

Back

Close

Full Screen / Esc

Printer-friendly Version

Interactive Discussion



data, the model optimisation is most sensitive on an intermediate time scale between one month and a year. During these time scales, the estimated cumulated discharge fractions of the more flexible TPLR and GM are almost similar. A comparison between the normalised and not normalised versions of the same model (see Fig. 5) suggests, that the tailings of the TFs did not seem to influence the predicted  $\delta^{18}\text{O}$  values or the objective function values at all.

This might help to explain the low identifiability of the TPLR model's parameter representing the mean transit time of the slow reservoir  $\tau_s$ . The long term tailing of a transfer function simply does not matter in respect to an objective function based on natural precipitation's  $\delta^{18}\text{O}$  in discharge. To assess this part of a catchment's TTD, a tracer with an extended temporal scope, like  $^3\text{H}$ , would be required. This was already emphasised by McDonnell et al. (2010), Stewart et al. (2010) and Stewart et al. (2012).

### 5.5 Meaningfulness of the mean transit time estimates

As mentioned in the previous section, a TTD containing longer transit times cannot be properly assessed solely with a cyclical annually varying environmental tracer like  $^{18}\text{O}$  or  $^2\text{H}$ . Still, it is possible to fit an arbitrary transfer function with any kind of long-term tailing to the measured environmental tracer data. A wide range of sufficiently flexible transfer functions is able to produce acceptable predictions of  $\delta^{18}\text{O}$  values in discharge. However, this is not enough to ensure an appropriate representation of a TTD's long-term behaviour. As the comparison of the not normalised and normalised variants of GM and TPLR in this study showed, the predicted long-term behaviour of the TTDs strongly affects MTT estimates without having any discernible impact on the predicted time series. Thus, reliable MTT estimates are not possible without the consideration of a tracer with extended temporal scope.

Even though the MTT estimates vary between the different model types (see Fig. 7), Fig. 8 indicates that the MTT estimates are not random, as there are significant, yet not very strong, correlations between most of the models' MTT estimates. It turns out that in respect to MTT estimates relying solely on stable water isotope data, TTP values

seem to be just as good as more complex convolution models: both can be used for a general classification into catchments with short, intermediate and long MTTs, neither can provide sound absolute values for MTT.

Given a sufficiently high measurement frequency, stable water isotope data seems to be suited to characterise the short term and intermediate part of a catchment's TTD, but it certainly does not contain enough information to determine complete TTDs or actual MTTs.

## 5.6 Relationship between MTT and topography

Despite the distinct differences between different model types' MTTs, the results in Table 4 suggest a significant correlation between MTTs (and the TTP) and the ratio  $L/G$  for most transfer functions.

McGuire et al. (2005) also reported a strong correlation between MTTs estimated by the EM and  $L/G$  for the *Lookout Creek* catchment and six of its subcatchments in the H. J. Andrews Experimental Forest in the central western Cascades of Oregon, USA. Tetzlaff et al. (2009b) likewise found the strongest correlation between MTTs and  $L/G$  for three Scottish catchments and their subcatchments, while the study of Hrachowitz et al. (2009) did not find a significant correlation between MTTs estimated by the GM and  $L/G$  for 20 catchments in the Scottish Highlands. Though, according to the method description in Hrachowitz et al. (2009) the stream network for all of the 20 Scottish catchments was computed with a fixed stream initiation threshold. At least for our study area, in some cases a fixed stream initiation threshold area caused large discrepancies between the computed and the observed channel networks and consequently led to different values for  $L$  as well as  $G$ . Therefore it cannot be excluded that Hrachowitz et al. (2009) found no significant correlation between MTTs and  $L/G$  because they worked with values for  $L$  and  $G$  which were derived with fixed stream initiation thresholds.

However, in this study most of the described correlations were only significant as long as the climatic influence of mean annual precipitation was not taken into account.

## Convolution models revisited

S. Seeger and M. Weiler

Title Page

Abstract

Introduction

Conclusions

References

Tables

Figures

⏪

⏩

◀

▶

Back

Close

Full Screen / Esc

Printer-friendly Version

Interactive Discussion



**Convolution models  
revisited**

S. Seeger and M. Weiler

[Title Page](#)[Abstract](#)[Introduction](#)[Conclusions](#)[References](#)[Tables](#)[Figures](#)[|◀](#)[▶|](#)[◀](#)[▶](#)[Back](#)[Close](#)[Full Screen / Esc](#)[Printer-friendly Version](#)[Interactive Discussion](#)

For most of the models, the correlation between MTTs and mean annual precipitation were higher than for any of the topographical indices. When two hypothetical catchments which share identical properties regarding geology, topography, soils and vegetation were considered, the catchment with the higher effective precipitation would undoubtedly expose higher turnover rates and hence lower MTTs. When the aim of a study is the assessment of the influence of catchment properties on MTTs, it would appear that it is necessary to first eliminate the influence of such first order climatic controls, i.e. to normalise MTTs by their respective mean annual precipitation. Yet, many studies (e.g. McGuire et al., 2005; Tetzlaff et al., 2009a, b; Hrachowitz et al., 2009; Soulsby et al., 2011; Mueller et al., 2013) did not account for this and directly compared MTTs of catchments with varying mean annual precipitation sums. This practice is likely to, at least partially, obscure the true influence of the (non-climatic) catchment properties. In this study, the mean annual precipitation normalised MTTs of different model types showed no consistent correlation to any topographic index, as significant correlations could be found or cancelled out by contemplating different subsets of catchments.

Due to collinearity between many of the topographic indices and the mean annual precipitation sums, the identification of crucial catchment properties is difficult and as long as the determination of the actual MTTs itself is uncertain (Which is the most appropriate model? How can the TTDs tailing properly assessed?), any method to regionalise MTTs will expose high degrees of uncertainty.

Similar to the work of Tetzlaff et al. (2009a), we suggest the combination of as many isotope tracer studies as possible to obtain a data set which, if sufficiently comprehensive, might be suited to compensate for the uncertainties in MTT estimations. Furthermore, to assess the influence of non climatic controls on tracer transit times, the consideration and neutralisation of mean effective precipitation sums is essential, as any direct comparison of MTTs will be dominated by the prevailing amounts of incoming water.

## 6 Conclusions

In this study, we used six different transfer models to estimate the TTDs and MTTs of 24 meso-scale catchments in Switzerland on the basis of  $\delta^{18}\text{O}$  data. We showed, that different transfer functions could be used to reach similarly acceptable fits to fortnightly sampled  $\delta^{18}\text{O}$  data in discharge. A comparison of the cumulated TTDs of those equally well performing models indicated that their cumulated values agreed at an intermediate time scale between three months and one year, while they diverged on shorter and even more so on longer time scales. From a certain point on, differences in TTD tailings did not influence the predicted  $\delta^{18}\text{O}$  values in discharge at all. Hence, to properly assess a catchment's TTD on all time scales, a higher sampling frequency of precipitation and discharge would be needed for more information on the catchment's short term behaviour and a more persistent tracer is required to determine the catchment's actual long term behaviour.

The poorly identifiable tailings of the TTDs greatly influenced MTT estimates, which partially exhibited high uncertainties. For catchments with longer MTTs, different model types' MTT estimates could differ by orders of magnitude while the available data was not suited to determine the most appropriate model type. In many cases the EM proved to be less appropriate than the more flexible GM and the TPLR. Given the fact, that the easily computable TTP values showed a good correlation to MTT estimates of most of the more complex transfer functions, they might serve as a coequal replacement for them, as long as the latter are as underdetermined as in this study and only relative differences among the catchments are the focus.

The results of this study suggest that seemingly good correlations between MTTs and the ratio of median flow path lengths over median flow path gradients  $L/G$  or the closely related drainage densities DD are mainly caused by the mean annual precipitation sums, which considerably influence these topographic indices as well as the MTTs. In order to assess the actual influence of topographic indices on

HESSD

11, 6753–6803, 2014

### Convolution models revisited

S. Seeger and M. Weiler

Title Page

Abstract

Introduction

Conclusions

References

Tables

Figures

◀

▶

◀

▶

Back

Close

Full Screen / Esc

Printer-friendly Version

Interactive Discussion



MTTs, the influence of the mean annual precipitation should be removed (normalised) beforehand.

## Appendix A: Technical considerations of convolution models

When a time  $t$  is inserted into a mathematically defined transfer function  $g(\tau)$  (see Table 2), the resulting value of the transfer function (from now on TF) belongs to exactly this point  $t$  in time. Model data, on the other hand, do not correspond to certain points in time, but rather to the time periods single model time steps are covering.

Furthermore, the sum of an infinite, equally spaced series of TF point values usually differs from unity, even when the curve of the TF itself integrates to unity, as is the case for all TFs shown in Table 2. However, for the sake of mass conservation, an, if necessary infinite, row of discrete model TF values eventually has to sum up to unity. This is usually achieved through normalisation, i.e. each of the discrete model TF values is divided by the total sum of all model TF values. Three issues arise from the practice described above:

- at the beginning of a steeply declining TF, the use of point based computations of TF values can lead to big deviations from a time step's average TF value (see left of Fig. A1)
- when a substantial part of the TF's tail exceeds the simulation period, normalisation to unity distorts the actual TF and redistributes a significant part of the signal to a place not defined by the TF's equation (see right side of Fig. A1)
- MTTs of normalised TFs cannot longer be computed analytically (right column of Table 2) and have to be inferred numerically

The first two issues, one caused by the point based TF value computation, the other caused by normalisation, cause the TF values used for modelling to deviate from the mathematically defined TF and make them depend on model time step length

## Convolution models revisited

S. Seeger and M. Weiler

Title Page

Abstract

Introduction

Conclusions

References

Tables

Figures



Back

Close

Full Screen / Esc

Printer-friendly Version

Interactive Discussion



and simulation period length. Both issues can be encountered by the same measure: instead of computing the value of the original transfer function  $g(\tau)$  for a certain point within time step  $t$ , the definite integral for  $g(\tau)$  has to be computed over the whole time step:

$$5 \quad G(t) = \int_{t-1}^t g(\tau) \quad (\text{A1})$$

This approach allows for an accurate computation of the average TF value over any model time step and is independent from model time step length and transfer function steepness. In the case of TFs which integrate to unity, it also eliminates the need for normalisation and therefore preserves long tailings of TFs which exceed the simulated time range.

## Appendix B: Validation of the interpolated precipitation isotope data

### B1 Origin of the validation data

15 Within the frame project of this study, bulk precipitation samples have been taken to determine the isotopic composition of the precipitation at five sites in Central Switzerland. With lengths of not more than one year and limited spatial coverage, these time series were of little use as model input data. Three of those sites, *Benglen*, *Schallenberg* and *Aeschau* have been chosen to validate the interpolated precipitation isotope data.

20 Further isotope composition data was thankfully obtained from Mueller et al. (2013), who collected precipitation bulk samples for the summer half years of 2010 and 2011 for four small alpine catchments in the Ursern Valley in southern Central Switzerland. Data from the two sites *Bonegg* and *Laubgaedem* were included into the validation data to extend the their elevation range up to 1720 m.

## Convolution models revisited

S. Seeger and M. Weiler

Title Page

Abstract

Introduction

Conclusions

References

Tables

Figures

⏪

⏩

◀

▶

Back

Close

Full Screen / Esc

Printer-friendly Version

Interactive Discussion



The Institute for Atmospheric and Climate Science (IAC) of the Swiss Federal Institute of Technology Zurich maintains the field measurement site *Messtelle Buel* within the catchment *Rietholzbach* for which fortnightly bulk sample data for  $\delta^{18}\text{O}$  from 1994 until the beginning of the year 2010 were available.

## B2 Reasons for the qualitative validation

The method described in Sect. 3.2 was not only applied to obtain precipitation isotope compositions for the studied catchments, but also for all available validation sites. Unfortunately, the temporal resolutions of the monthly interpolation derived predictions and the sub-monthly observed  $\delta^{18}\text{O}$  time series were not the same. To aggregate isotope composition data to a coarser time scale, mass weighted averaging would be required, but the respective precipitation amounts to the bulk sample isotope data were not available. Hence, a quantitative validation of the interpolation based predictions was not possible, instead a qualitative comparison was made.

## B3 Comparison of predictions and validation data

Figure B1 shows the monthly predicted  $\delta^{18}\text{O}$  values obtained by the interpolation procedure described in Sect. 3.2 plotted with the on-site measured validation data. All validation time series have been collected over shorter periods than one month and thus exhibit more variance and higher amplitudes than the monthly predictions. Nevertheless, a qualitative comparison of predicted and validation data indicates a reasonably well performance of the interpolation method.

*Acknowledgements.* This work has been funded as part of the National Research Programme NRP 61 by the Swiss National Science Foundation. We are grateful to Massimiliano Zappa from the Swiss Federal Institute for Forest, Snow and Landscape Research WSL, who provided the preprocessed PREVAH-climate data and Manfred Stähli (WSL) for discharge data on the catchments *Vogelbach*, *Erlenbach* and *Luempenenbach*. Furthermore we would like to thank Matthias H. Mueller (University of Basel) of for the provision of supplemental precipitation

HESSD

11, 6753–6803, 2014

## Convolution models revisited

S. Seeger and M. Weiler

Title Page

Abstract

Introduction

Conclusions

References

Tables

Figures

◀

▶

◀

▶

Back

Close

Full Screen / Esc

Printer-friendly Version

Interactive Discussion



isotope data. The article processing charge was funded by the German Research Foundation (DFG) and the Albert Ludwigs University Freiburg in the funding programme Open Access Publishing.

## References

- 5 Beven, K. J. and Binley, A.: The future of distributed models: model calibration and uncertainty prediction, *Hydrol. Process.*, 6, 279–298, doi:10.1002/hyp.3360060305, 1992. 6766
- Birkel, C., Soulsby, C., Tetzlaff, D., Dunn, S. M., and Spezia, L.: High-frequency storm event isotope sampling reveals time-variant transit time distributions and influence of diurnal cycles, *Hydrol. Process.*, 26, 308–316, doi:10.1002/hyp.8210, 2012. 6764
- 10 Böhner, J. and Selige, T.: Spatial prediction of soil attributes using terrain analysis and climate regionalisation, *Göttinger Geographische Abhandlungen*, 115, 13–28, available at: <http://www.saga-gis.org/en/about/references.html>, last access: 12 February 2014, 2006. 6760
- Capell, R., Tetzlaff, D., Hartley, A. J., and Soulsby, C.: Linking metrics of hydrological function and transit times to landscape controls in a heterogeneous mesoscale catchment, *Hydrol. Process.*, 26, 405–420, doi:10.1002/hyp.8139, 2012. 6755, 6756, 6764
- 15 Conrad, O., Wichmann, V., Olaya, V., and Ringeler, A.: SAGA GIS (version 2.1), <http://www.saga-gis.org>, last access: 6 May 2014, 2013. 6759
- Deb, K., Pratap, A., Agarwal, S., and Meyarivan, T.: A fast and elitist multiobjective genetic algorithm: NSGA-II, *IEEE Transactions on Evolutionary Computation*, 6, 182–197, doi:10.1109/4235.996017, 2002. 6765
- 20 Delhomme, J. P.: Kriging in the hydrosociences, *Adv. Water Resour.*, 1, 251–266, doi:10.1016/0309-1708(78)90039-8, 1978. 6760
- DeWalle, D. and Edwards, P.: Seasonal isotope hydrology of three Appalachian forest catchments, *Hydrol. Process.*, 11, 1895–1906, 1997. 6761
- 25 Gupta, H. V., Kling, H., Yilmaz, K. K., and Martinez, G. F.: Decomposition of the mean squared error and NSE performance criteria: implications for improving hydrological modelling, *J. Hydrol.*, 377, 80–91, doi:10.1016/j.jhydrol.2009.08.003, 2009. 6765, 6766
- Heidbüchel, I., Troch, P. A., Lyon, S. W., and Weiler, M.: The master transit time distribution of variable flow systems, *Water Resour. Res.*, 48, W06520, doi:10.1029/2011WR011293, 30 2012. 6755, 6764

## Convolution models revisited

S. Seeger and M. Weiler

Title Page

Abstract

Introduction

Conclusions

References

Tables

Figures

⏪

⏩

◀

▶

Back

Close

Full Screen / Esc

Printer-friendly Version

Interactive Discussion



**Convolution models  
revisited**

S. Seeger and M. Weiler

[Title Page](#)[Abstract](#)[Introduction](#)[Conclusions](#)[References](#)[Tables](#)[Figures](#)[⏪](#)[⏩](#)[◀](#)[▶](#)[Back](#)[Close](#)[Full Screen / Esc](#)[Printer-friendly Version](#)[Interactive Discussion](#)

- Hrachowitz, M., Soulsby, C., Tetzlaff, D., Dawson, J. J. C., and Malcolm, I. A.: Regionalization of transit time estimates in montane catchments by integrating landscape controls, *Water Resour. Res.*, 45, W05421, doi:10.1029/2008WR007496, 2009. 6756, 6777, 6778
- 5 Hrachowitz, M., Soulsby, C., Tetzlaff, D., Malcolm, I. A., and Schoups, G.: Gamma distribution models for transit time estimation in catchments: physical interpretation of parameters and implications for time-variant transit time assessment, *Water Resour. Res.*, 46, W10536, doi:10.1029/2010WR009148, 2010. 6755, 6764
- Hrachowitz, M., Savenije, H., Bogaard, T. A., Tetzlaff, D., and Soulsby, C.: What can flux tracking teach us about water age distribution patterns and their temporal dynamics?, *Hydrol. Earth Syst. Sci.*, 17, 533–564, doi:10.5194/hess-17-533-2013, 2013. 6755
- 10 Jakeman, A. J. and Hornberger, G.: How much complexity is warranted in a rainfall-runoff model?, *Water Resour. Res.*, 29, 2637–2649, doi:10.1029/93WR00877, 1993. 6763, 6767, 6773
- Kirchner, J. W., Feng, X., and Neal, C.: Fractal stream chemistry and its implications for contaminant transport in catchments, *Nature*, 403, 524–7, doi:10.1038/35000537, 2000. 6764
- 15 Kling, H., Fuchs, M., and Paulin, M.: Runoff conditions in the upper Danube basin under an ensemble of climate change scenarios, *J. Hydrol.*, 424–425, 264–277, doi:10.1016/j.jhydrol.2012.01.011, 2012. 6765
- 20 Lyon, S. W., Laudon, H., Seibert, J., Mörth, M., Tetzlaff, D., and Bishop, K. H.: Controls on snowmelt water mean transit times in northern boreal catchments, *Hydrol. Process.*, 24, 1672–1684, doi:10.1002/hyp.7577, 2010. 6755
- Małoszewski, P. and Zuber, A.: Determining the turnover time of groundwater systems with the aid of environmental tracers, *J. Hydrol.*, 57, 207–231, 1982. 6755, 6764
- 25 Małoszewski, P., Rauert, W., Stichler, W., and Herrmann, A.: Application of flow models in an alpine catchment area using tritium and deuterium data, *J. Hydrol.*, 66, 319–330, doi:10.1016/0022-1694(83)90193-2, 1983. 6755
- McDonnell, J. J., McGuire, K. J., Aggarwal, P. K., Beven, K. J., Biondi, D., Destouni, G., Dunn, S. M., James, A., Kirchner, J. W., Kraft, P., Lyon, S. W., Maloszewski, P., Newman, B., Pfister, L., Rinaldo, A., Rodhe, A., Sayama, T., Seibert, J., Solomon, K., Soulsby, C., Stewart, M. K., Tetzlaff, D., Tobin, C., Troch, P. A., Weiler, M., Western, A., Wörman, A., and Wrede, S.: How old is streamwater? Open questions in catchment

**Convolution models  
revisited**

S. Seeger and M. Weiler

[Title Page](#)[Abstract](#)[Introduction](#)[Conclusions](#)[References](#)[Tables](#)[Figures](#)[I◀](#)[▶I](#)[◀](#)[▶](#)[Back](#)[Close](#)[Full Screen / Esc](#)[Printer-friendly Version](#)[Interactive Discussion](#)

transit time conceptualization, modelling and analysis, *Hydrol. Process.*, 24, 1745–1754, doi:10.1002/hyp.7796, 2010. 6776

McGuire, K. J.: The role of topography on catchment-scale water residence time, *Water Resour. Res.*, 41, W05002, doi:10.1029/2004WR003657, 2005. 6764

5 McGuire, K. J. and McDonnell, J. J.: A review and evaluation of catchment transit time modeling, *J. Hydrol.*, 330, 543–563, doi:10.1016/j.jhydrol.2006.04.020, 2006. 6755

McGuire, K. J., McDonnell, J. J., Weiler, M., Kendall, C., McGlynn, B. L., Welker, J. M., and Seibert, J.: The role of topography on catchment-scale water residence time, *Water Resour. Res.*, 41, W05002, doi:10.1029/2004WR003657, 2005. 6756, 6777, 6778

10 Mueller, M. H., Weingartner, R., and Alewell, C.: Importance of vegetation, topography and flow paths for water transit times of base flow in alpine headwater catchments, *Hydrol. Earth Syst. Sci.*, 17, 1661–1679, doi:10.5194/hess-17-1661-2013, 2013. 6755, 6756, 6764, 6767, 6778, 6781

Pebesma, E. J.: Multivariable geostatistics in S: the gstat package, *Comput. Geosci.*, 30, 683–691, doi:10.1016/j.cageo.2004.03.012, 2004. 6760

Roa-García, M. C. and Weiler, M.: Integrated response and transit time distributions of watersheds by combining hydrograph separation and long-term transit time modeling, *Hydrol. Earth Syst. Sci.*, 14, 1537–1549, doi:10.5194/hess-14-1537-2010, 2010. 6755, 6764

15 Sicart, J. and Hock, R.: Sky longwave radiation on tropical Andean glaciers: parameterization and sensitivity to atmospheric variables, *J. Glaciol.*, 56, 854–860, doi:10.3189/002214310794457182, 2010. 6762

Siegenthaler, U. and Oeschger, H.: Correlation of  $^{18}\text{O}$  in precipitation with temperature and altitude, *Nature*, 285, 317, doi:10.1038/285314a0, 1980. 6767

20 Soulsby, C. and Tetzlaff, D.: Towards simple approaches for mean residence time estimation in ungauged basins using tracers and soil distributions, *J. Hydrol.*, 363, 60–74, doi:10.1016/j.jhydrol.2008.10.001, 2008. 6755, 6756

Soulsby, C., Piegat, K., Seibert, J., and Tetzlaff, D.: Catchment-scale estimates of flow path partitioning and water storage based on transit time and runoff modelling, *Hydrol. Process.*, 25, 3960–3976, doi:10.1002/hyp.8324, 2011. 6755, 6764, 6778

30 Stewart, M. K. and McDonnell, J. J.: Modeling base flow soil water residence times from deuterium concentrations, *Water Resour. Res.*, 27, 2681–2693, doi:10.1029/91WR01569, 1991. 6764

**Convolution models  
revisited**

S. Seeger and M. Weiler

Title Page

Abstract

Introduction

Conclusions

References

Tables

Figures

I◀

▶I

◀

▶

Back

Close

Full Screen / Esc

Printer-friendly Version

Interactive Discussion



Stewart, M. K., Morgenstern, U., and McDonnell, J. J.: Truncation of stream residence time: how the use of stable isotopes has skewed our concept of streamwater age and origin, *Hydrol. Process.*, 24, 1646–1659, doi:10.1002/hyp.7576, 2010. 6776

Stewart, M. K., Morgenstern, U., McDonnell, J. J., and Pfister, L.: The “hidden streamflow” challenge in catchment hydrology: a call to action for stream water transit time analysis, *Hydrol. Process.*, 26, 2061–2066, doi:10.1002/hyp.9262, 2012. 6776

Strasser, U. and Marke, T.: *ESCIMO.spread* – a spreadsheet-based point snow surface energy balance model to calculate hourly snow water equivalent and melt rates for historical and changing climate conditions, *Geosci. Model Dev.*, 3, 643–652, doi:10.5194/gmd-3-643-2010, 2010. 6762

Taylor, S., Feng, X., Kirchner, J. W., Osterhuber, R., Klaue, B., and Renshaw, C. E.: Isotopic evolution of a seasonal snowpack and its melt, *Water Resour. Res.*, 37, 759–769, doi:10.1029/2000WR900341, 2001. 6774

Tetzlaff, D., Seibert, J., McGuire, K. J., Laudon, H., Burns, D. A., Dunn, S. M., and Soulsby, C.: How does landscape structure influence catchment transit time across different geomorphic provinces?, *Hydrol. Process.*, 23, 945–953, doi:10.1002/hyp.7240, 2009a. 6756, 6761, 6762, 6778

Tetzlaff, D., Seibert, J., and Soulsby, C.: Inter-catchment comparison to assess the influence of topography and soils on catchment transit times in a geomorphic province; the Cairngorm mountains, Scotland, *Hydrol. Process.*, 1886, 1874–1886, doi:10.1002/hyp.7318, 2009b. 6755, 6756, 6777, 6778

Trautmann, H., Steuer, D., and Mersmann, O.: mco: Multi criteria optimization algorithms and related functions, <http://cran.r-project.org/package=mco> (last access: 7 October 2013, 2013. 6765

Unnikrishna, P., McDonnell, J. J., and Kendall, C.: Isotope variations in a Sierra Nevada snowpack and their relation to meltwater, *J. Hydrol.*, 260, 38–57, doi:10.1016/S0022-1694(01)00596-0, 2002. 6774

Viviroli, D., Zappa, M., Gurtz, J., and Weingartner, R.: An introduction to the hydrological modelling system PREVAH and its pre- and post-processing-tools, *Environ. Modell. Softw.*, 24, 1209–1222, doi:10.1016/j.envsoft.2009.04.001, 2009a. 6758

Viviroli, D., Zappa, M., Schwanbeck, J., Gurtz, J., and Weingartner, R.: Continuous simulation for flood estimation in ungauged mesoscale catchments of Switzerland

– Part I: Modelling framework and calibration results, J. Hydrol., 377, 191–207, doi:10.1016/j.jhydrol.2009.08.023, 2009b. 6758

Weiler, M.: How does rainfall become runoff? A combined tracer and runoff transfer function approach, Water Resour. Res., 39, 1315, doi:10.1029/2003WR002331, 2003. 6762, 6763, 6764, 6773

5

# HESSD

11, 6753–6803, 2014

## Convolution models revisited

S. Seeger and M. Weiler

Title Page

Abstract

Introduction

Conclusions

References

Tables

Figures



Back

Close

Full Screen / Esc

Printer-friendly Version

Interactive Discussion



Convolution models  
revisited

S. Seeger and M. Weiler

**Table 1.** Areas, elevations, and mean annual precipitation sums of the 24 studied catchments.

catchment name	gauging station	catchment ID	area [km <sup>2</sup> ]	mean elev. [m]	min elev. [m]	max elev. [m]	prcp [mm a <sup>-1</sup> ]
Dischmabach	Davos	DIS	43.2	2369	1663	3139	1391
Ova da Cluozza	Zernez	OVA	26.9	2364	1519	3160	1053
Riale di Calneggia	Cavergno	RIA	23.9	1986	881	2908	2104
Allenbach	Adelboden	ALL	28.8	1852	1293	2742	1651
Schaechen	Buerglen	SCH	107.9	1719	487	3260	1687
Sitter	Appenzell	SIT	88.2	1301	768	2500	1870
Biber	Biberbrugg	BIB	31.6	999	827	1495	1639
Alp	Einsiedeln	ALP	46.5	1154	845	1894	2112
Luempfenbach	–	ALP_L	0.9	1336	1092	1508	2615
Erlenbach	–	ALP_E	0.7	1359	1117	1650	2168
Vogelbach	–	ALP_V	1.6	1335	1038	1540	2161
Sense	Thoerishaus	SEN	351.2	1068	554	2184	1270
Ilfis	Langnau	ILF	187.9	1037	681	2087	1450
Emme	Eggiwil	EMM	127	1285	743	2216	1559
Roethebach	Eggiwil	ROE	54.1	991	731	1542	1099
Guerbe	Burgstein	GUE	55.4	1037	556	2152	1241
Mentue	Yvonand	MEN	105.0	679	447	926	1060
Langeten	Huttwil	LAN	60.3	760	598	1100	1195
Aach	Salmsach	AAC	50.0	472	408	560	1095
Ergolz	Liestal	ERG	261.2	584	305	1165	1012
Aabach	Moenchaltorf	AAB	55.6	635	519	1092	1081
Murg	Waengi	MUR	76.8	648	467	1036	1281
Rietholzbach	Mosnang	RIE	3.2	794	671	938	1555
Oberer Rietholzbach	–	RIE_O	0.9	815	748	938	1670

Title Page

Abstract

Introduction

Conclusions

References

Tables

Figures

I◀

▶I

◀

▶

Back

Close

Full Screen / Esc

Printer-friendly Version

Interactive Discussion



Convolution models  
revisited

S. Seeger and M. Weiler

**Table 2.** Overview of transfer functions with specification of the parameters and analytical mean transit time (MTT).

Transfer function	Parameters	analytical MTT
Linear reservoir (EM) $g(\tau) = \frac{1}{\tau_m} \exp\left(-\frac{\tau}{\tau_m}\right)$	$\tau_m$ mean transit time	$\tau_m$
Gamma Distribution (GM) $g(\tau) = \frac{\tau^{\alpha-1}}{\beta^\alpha \Gamma(\alpha)} \exp(-\tau/\beta)$	$\alpha$ shape parameter $\beta$ scale parameter	$\alpha\beta$
Two parallel linear reservoirs (TPLR) $h(\tau) = g(\tau) = \frac{\phi}{\tau_f} \exp\left(-\frac{\tau}{\tau_f}\right) + \frac{1-\phi}{\tau_s} \exp\left(-\frac{\tau}{\tau_s}\right)$	$\phi$ fraction of fast reservoir $\tau_f$ MTT of fast reservoir $\tau_s$ MTT of slow reservoir	$\phi\tau_f + (1 - \phi)\tau_s$

Title Page

Abstract

Introduction

Conclusions

References

Tables

Figures

I ◀

▶ I

◀

▶

Back

Close

Full Screen / Esc

Printer-friendly Version

Interactive Discussion



**Table 3.** Results of the topographic analysis.  $L$  is the flowpath length,  $G$  the flow gradient, DD the drainage densities and TWI the topographic wetness index.

catchment ID	$L$ [m]	$G$ [ $\text{m m}^{-1}$ ]	$L/G$ [m]	DD [ $\text{m m}^{-2}$ ]	TWI [-]
DIS	647	0.33	1961	0.024	9.52
OVA	616	0.46	1339	0.020	8.87
RIA	647	0.46	1407	0.025	9.10
ALL	423	0.31	1365	0.033	9.27
SCH	646	0.38	1700	0.023	9.38
SIT	329	0.27	1219	0.045	9.48
BIB	207	0.16	1294	0.060	9.96
ALP	196	0.21	933	0.079	9.69
ALP_L	155	0.17	912	0.098	9.61
ALP_E	169	0.20	845	0.104	9.67
ALP_V	193	0.28	689	0.070	9.22
SEN	227	0.20	1135	0.056	9.76
ILF	157	0.30	523	0.075	9.00
EMM	286	0.27	1059	0.046	9.43
ROE	210	0.18	1167	0.050	9.67
GUE	258	0.19	1358	0.065	9.88
MEN	364	0.08	4550	0.028	10.83
LAN	308	0.11	2800	0.030	9.85
AAC	481	0.02	24 050	0.026	11.67
ERG	421	0.15	2807	0.022	9.99
AAB	407	0.04	10 175	0.032	10.92
MUR	219	0.10	2190	0.049	10.07
RIE	194	0.18	1078	0.056	9.51
RIE_O	254	0.15	1693	0.043	9.46

## Convolution models revisited

S. Seeger and M. Weiler

Title Page

Abstract

Introduction

Conclusions

References

Tables

Figures



Back

Close

Full Screen / Esc

Printer-friendly Version

Interactive Discussion



## Convolution models revisited

S. Seeger and M. Weiler

**Table 4.** Correlation coefficients of different model types' MTTs and the transit time proxy (TTP) to topographic indices and mean annual precipitation sums. Pearson correlation coefficients are given as  $r$ , Spearman rank correlation coefficients are given as  $\rho$ . Significant correlations ( $\rho$  value < 0.05) are printed in boldface, correlations with  $\rho$  values  $\geq 0.2$  are printed in italics.

model	area		elevation		L		G		L/G		DD		TWI		prcp	
	$r$	$\rho$	$r$	$\rho$	$r$	$\rho$	$r$	$\rho$	$r$	$\rho$	$r$	$\rho$	$r$	$\rho$	$r$	$\rho$
all 24 catchments																
EM	<i>0.24</i>	0.29	-0.16	-0.26	0.06	0.17	-0.1	-0.12	-0.06	0.33	-0.38	-0.32	-0.1	0	<b>-0.47</b>	-0.39
EM*	0.18	0.19	-0.12	-0.19	0.01	0.1	-0.05	-0.04	-0.1	0.21	-0.29	-0.24	-0.19	-0.11	-0.36	-0.26
GM	0.22	0.38	<b>-0.43</b>	<b>-0.53</b>	0.01	0.14	<b>-0.46</b>	<b>-0.46</b>	0.08	<b>0.5</b>	-0.4	-0.36	0.31	0.31	<b>-0.61</b>	<b>-0.7</b>
GM*	0.26	0.26	-0.2	-0.4	0.06	0.18	-0.24	-0.33	-0.01	<b>0.45</b>	<b>-0.42</b>	-0.38	0.06	0.17	<b>-0.63</b>	<b>-0.59</b>
TPLR	0.1	0.08	0.12	-0.17	0.18	0.24	-0.08	-0.23	-0.06	<b>0.42</b>	-0.32	<b>-0.42</b>	0.03	0.16	-0.32	-0.5
TPLR*	0.08	0.1	-0.13	-0.34	0.09	0.24	-0.27	-0.32	0.26	<b>0.42</b>	-0.3	<b>-0.45</b>	0.23	0.2	<b>-0.51</b>	<b>-0.68</b>
TTP	0.06	0.27	-0.16	-0.28	0.06	0.28	-0.17	-0.14	-0.06	<b>0.47</b>	-0.37	<b>-0.45</b>	-0.03	0.05	<b>-0.43</b>	<b>-0.53</b>
without <i>Mentue</i> , <i>Aabach</i> and <i>Aach</i>																
EM	0.25	0.35	-0.3	<b>-0.5</b>	0.11	0.29	-0.3	-0.38	<b>0.63</b>	<b>0.63</b>	<b>-0.5</b>	<b>-0.48</b>	0.18	0.19	<b>-0.67</b>	<b>-0.66</b>
EM*	0.21	0.32	-0.33	<b>-0.51</b>	0.07	0.26	-0.32	-0.38	<b>0.6</b>	<b>0.61</b>	<b>-0.47</b>	<b>-0.46</b>	0.16	0.15	<b>-0.63</b>	<b>-0.65</b>
GM	0.23	0.33	-0.42	<b>-0.51</b>	-0.01	0.12	<b>-0.46</b>	-0.42	<b>0.77</b>	<b>0.48</b>	-0.38	-0.38	0.39	0.22	<b>-0.62</b>	<b>-0.72</b>
GM*	0.25	0.28	-0.2	-0.42	0.07	0.22	-0.26	-0.37	<b>0.52</b>	<b>0.55</b>	<b>-0.44</b>	<b>-0.45</b>	0.09	0.19	<b>-0.67</b>	<b>-0.67</b>
TPLR	0.07	0.06	0.12	-0.14	0.21	0.23	-0.13	-0.22	<b>0.52</b>	<b>0.46</b>	-0.35	<b>-0.44</b>	0.13	0.13	-0.36	<b>-0.54</b>
TPLR*	0.09	0.04	-0.01	-0.22	0.03	0.07	-0.14	-0.17	0.32	0.22	-0.23	-0.33	-0.03	-0.03	<b>-0.45</b>	<b>-0.6</b>
TTP	0.06	0.29	-0.25	-0.38	0.1	0.34	-0.31	-0.24	<b>0.7</b>	<b>0.64</b>	<b>-0.44</b>	<b>-0.52</b>	0.22	0.14	<b>-0.55</b>	<b>-0.66</b>
all 24 catchments (MTTs normalised by mean annual precipitation sums)																
EM	-0.06	-0.03	0.32	0.22	0.21	0.17	0.3	0.28	-0.29	0.08	-0.23	-0.24	<b>-0.44</b>	<b>-0.43</b>	0.07	0.11
EM*	-0.08	-0.05	0.27	0.28	0.14	0.11	0.27	0.32	-0.28	-0.01	-0.17	-0.16	<b>-0.46</b>	<b>-0.47</b>	0.1	0.18
GM	0.08	0.23	-0.21	-0.31	0.04	0.15	-0.31	-0.3	-0.03	<b>0.43</b>	-0.35	-0.34	0.1	0.12	<b>-0.46</b>	<b>-0.46</b>
GM*	-0.04	-0.05	0.22	0.03	0.09	0.03	0.09	0.04	-0.2	0.09	-0.21	-0.19	-0.28	-0.27	-0.14	-0.17
TPLR	-0.19	-0.11	0.37	0.05	0.05	0.03	0.11	-0.04	-0.17	0.11	0.05	-0.19	-0.19	-0.1	0.24	-0.22
TPLR*	-0.4	<b>-0.7</b>	<b>0.43</b>	<b>0.52</b>	-0.09	-0.18	0.24	0.36	-0.24	-0.4	0.35	0.19	-0.37	<b>-0.51</b>	<b>0.58</b>	<b>0.5</b>
TTP	-0.25	-0.27	0.36	0.38	0.17	-0.03	0.28	0.36	-0.34	-0.11	-0.16	-0.04	<b>-0.45</b>	<b>-0.52</b>	0.18	0.39
without <i>Mentue</i> , <i>Aabach</i> and <i>Aach</i> (MTTs normalised by mean annual precipitation sums)																
EM	-0.08	0.02	0.16	0	0.33	0.31	0.07	0.03	0.34	<b>0.45</b>	-0.43	-0.43	-0.19	-0.25	-0.14	-0.16
EM*	-0.1	0.02	0.09	0.02	0.26	0.29	0.01	0.03	0.32	0.41	-0.39	-0.39	-0.18	-0.24	-0.13	-0.14
GM	0.07	0.18	-0.23	-0.37	0.05	0.16	-0.36	-0.34	<b>0.67</b>	<b>0.49</b>	-0.38	-0.41	0.24	0.08	<b>-0.5</b>	<b>-0.51</b>
GM*	-0.05	-0.07	0.14	-0.07	0.15	0.09	-0.03	-0.07	0.24	0.24	-0.31	-0.3	-0.18	-0.23	-0.25	-0.29
TPLR	-0.21	-0.14	0.33	0.04	0.1	0.07	0.01	-0.12	0.09	0.22	0	-0.25	-0.08	-0.04	0.19	-0.29
TPLR*	-0.42	<b>-0.72</b>	0.37	<b>0.47</b>	-0.04	-0.13	0.12	0.26	-0.27	-0.26	0.29	0.12	-0.31	<b>-0.44</b>	<b>0.54</b>	<b>0.44</b>
TTP	-0.29	-0.24	0.2	0.11	0.3	0.15	0.03	0.04	0.43	0.32	-0.36	-0.27	-0.14	-0.28	-0.02	0.12

Title Page

Abstract Introduction

Conclusions References

Tables Figures

◀ ▶

◀ ▶

Back Close

Full Screen / Esc

Printer-friendly Version

Interactive Discussion



**Table 5.** Minimum, median and maximum MTT in years for each catchment and transfer function type and the respective transit time proxy (TTP) values.

catchment	GM			TPLR			EM			GM*			TPLR*			EM*			TTP
	min	med	max	min	med	max	min	med	max										
DIS	9.16	10.5	12	84.5	96.7	102	1.42	1.51	1.54	5.67	5.73	5.78	8.18	8.39	8.49	1.43	1.49	1.57	12.60
OVA	3.32	4.81	8.46	32.1	67.7	94.9	0.87	0.91	0.94	2.54	3.88	4.73	7.09	7.5	7.69	0.87	0.9	0.94	7.46
RIA	0.43	0.6	0.75	0.65	1.79	72.7	0.45	0.57	0.68	0.41	0.59	1.05	0.96	4.02	5.25	0.44	0.57	0.68	4.59
ALL	4.33	6.25	8.65	22.3	70.5	108	1.53	1.58	1.65	4.1	5.06	5.39	4.16	5.44	8.17	1.55	1.55	1.66	8.90
SCH	1.11	1.21	1.25	1.11	1.2	1.27	1.11	1.2	1.26	1.08	1.18	1.24	1.09	1.2	2.3	1.13	1.18	1.21	7.16
SIT	0.69	0.92	1.7	0.79	0.9	68	0.61	0.68	0.74	0.66	0.9	1.43	0.81	0.87	5.48	0.61	0.66	0.72	4.40
BIB	0.52	0.76	1.23	0.78	8.49	71.6	0.3	0.36	0.4	0.52	0.72	1.08	0.76	4.53	5.34	0.32	0.37	0.41	4.59
ALP	0.35	0.46	0.57	0.58	0.8	35	0.24	0.28	0.32	0.35	0.47	0.75	3.33	4.02	4.45	0.22	0.28	0.32	3.91
ALP_L	1.7	1.91	2.24	18.5	65.7	80.8	0.52	0.55	0.59	1.44	1.76	2	5.28	5.63	6	0.53	0.55	0.6	4.68
ALP_E	0.14	0.21	0.35	0.52	0.57	1.51	0.15	0.17	0.18	0.16	0.21	0.33	2.43	3.35	4.08	0.12	0.17	0.19	2.61
ALP_V	0.66	1.02	1.48	1.47	47.3	78.8	0.18	0.27	0.35	0.66	0.95	1.56	3.57	5.37	5.86	0.23	0.29	0.35	4.30
SEN	2.36	5.82	17.6	3.13	39	84	1.25	1.34	1.43	2.72	4.13	4.64	2.82	5.91	6.8	1.25	1.34	1.41	5.31
ILF	5.31	8.88	20.7	3.62	12.1	88.6	1.49	1.55	1.75	4.07	5.05	5.32	3.12	6.36	7.91	1.41	1.61	1.68	9.13
EMM	1.14	1.66	2.77	3.18	12.3	71.5	0.39	0.42	0.48	1.08	1.41	2.23	4.24	5.16	5.69	0.37	0.43	0.48	3.99
ROE	6.5	12.2	25.6	5.31	59.5	108	0.29	1.77	2.45	4.25	5.22	5.56	1.98	6.54	8.11	1.15	1.74	2.12	9.54
GUE	1.04	1.33	2.52	1.43	5.55	75.4	0.84	1.04	1.15	1.05	1.35	2.48	1.64	3.93	5.26	0.94	1.06	1.15	5.50
MEN	12.9	18.2	20.7	23.7	69.3	105	0.02	0.86	1.84	3.96	4.43	4.85	6.19	6.83	7.29	0.02	0.08	1.85	5.21
LAN	20.4	29	31.8	21.6	67.2	122	2.17	2.31	2.36	5.91	6.07	6.18	7.62	8.42	8.7	2.16	2.31	2.43	15.00
AAC	1.05	1.6	2.96	1.72	19.6	98.7	0.76	1.03	1.1	1.13	1.79	2.91	3.3	6.76	7.22	0.75	1	1.12	4.65
ERG	7.42	18.8	29	18.2	81.4	114	1.45	1.63	1.86	4.59	5.53	5.83	3.49	7.32	8.25	1.51	1.63	1.81	9.34
AAB	11.7	18.5	21.6	4.28	17.2	105	0.01	0.09	2.36	3.76	4.49	4.85	5.39	7.24	7.91	0.04	0.05	1.21	5.71
MUR	12.4	20.5	26.4	8.79	74	112	1.71	1.79	1.82	4.89	5.3	5.46	2.68	4.07	7.18	1.7	1.78	1.87	10.75
RIE	2.45	6.44	14.3	4.05	15.8	68.9	0.79	1.34	2.02	3.14	4.76	5.48	4.84	6.01	7.16	0.8	1.41	2.12	7.26
RIE_O	2.02	8.44	26.4	3.1	21.9	100	0.91	2.02	4.04	1.86	5.29	6.45	3.31	6.28	8.22	0.84	2.44	3.96	8.95

Title Page

Abstract

Introduction

Conclusions

References

Tables

Figures

◀

▶

◀

▶

Back

Close

Full Screen / Esc

Printer-friendly Version

Interactive Discussion



## Convolution models revisited

S. Seeger and M. Weiler

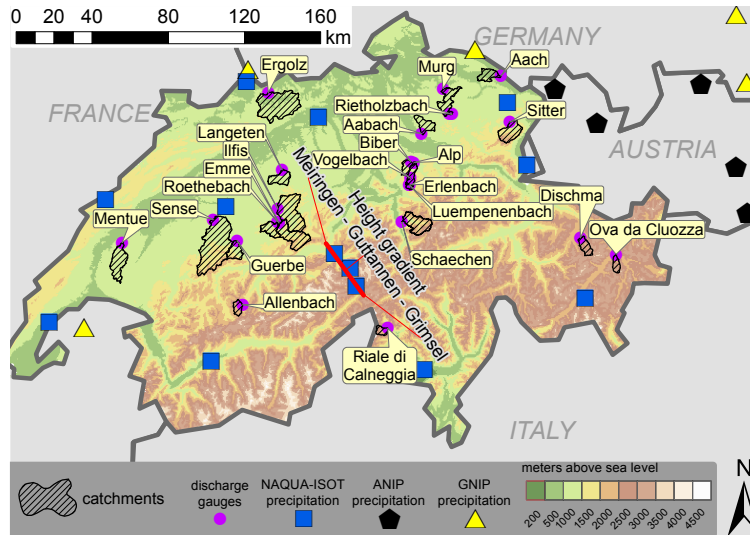


**Figure 1.** Map of the study area with elevation and catchment borders. The not shown catchment *Oberer Rietholzbach* is a subcatchment of the *Rietholzbach*-catchment. The symbols indicate positions of isotope measurement sites of various sources.

Title Page

Abstract	Introduction
Conclusions	References
Tables	Figures

⏪
⏩

◀
▶

Back
Close

Full Screen / Esc

Printer-friendly Version

Interactive Discussion



## Convolution models revisited

S. Seeger and M. Weiler

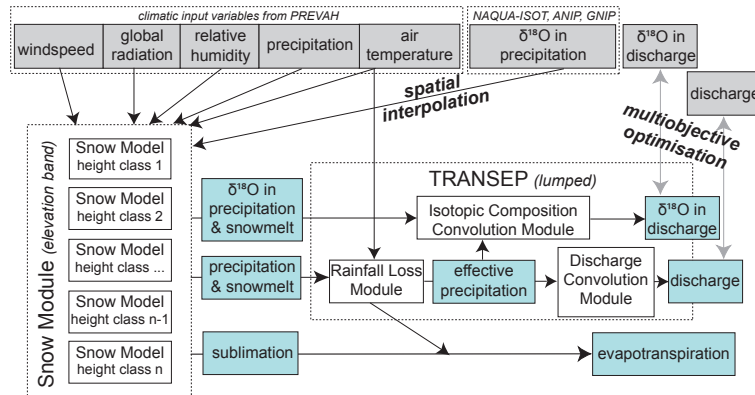


**Figure 2.** Overview scheme of the model modules. Grey boxes represent input data, blue boxes represent data computed by model modules (white boxes).

Title Page

Abstract Introduction

Conclusions References

Tables Figures

◀ ▶

◀ ▶

Back Close

Full Screen / Esc

Printer-friendly Version

Interactive Discussion



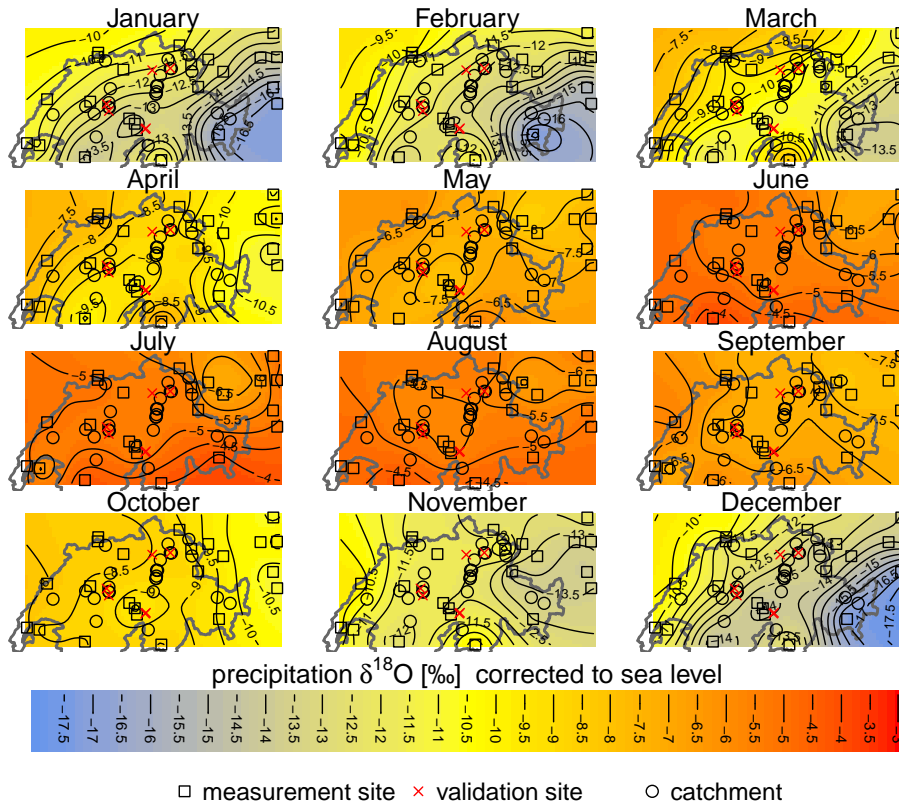


**Figure 3.** Monthly maps of interpolated sea level precipitation  $\delta^{18}\text{O}$  values.

[Title Page](#)  
[Abstract](#)   [Introduction](#)  
[Conclusions](#)   [References](#)  
[Tables](#)   [Figures](#)  
◀   ▶  
◀   ▶  
[Back](#)   [Close](#)  
[Full Screen / Esc](#)  
[Printer-friendly Version](#)  
[Interactive Discussion](#)



## Convolution models revisited

S. Seeger and M. Weiler

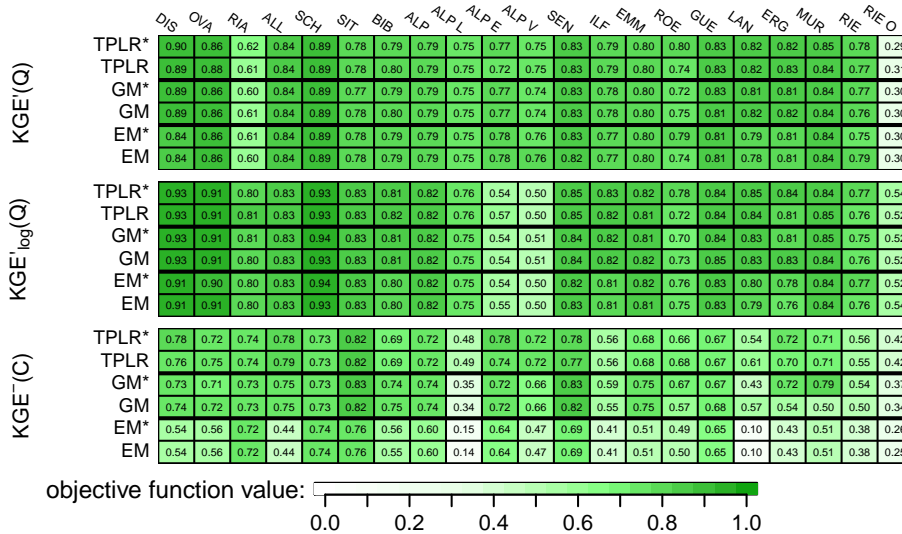


**Figure 4.** Values of the three objective functions for all catchments for the six different transfer functions. Asterisks mark normalised transfer functions.

[Title Page](#)

[Abstract](#)   [Introduction](#)

[Conclusions](#)   [References](#)

[Tables](#)   [Figures](#)

[◀](#)   [▶](#)

[◀](#)   [▶](#)

[Back](#)   [Close](#)

[Full Screen / Esc](#)

[Printer-friendly Version](#)

[Interactive Discussion](#)



## Convolution models revisited

S. Seeger and M. Weiler

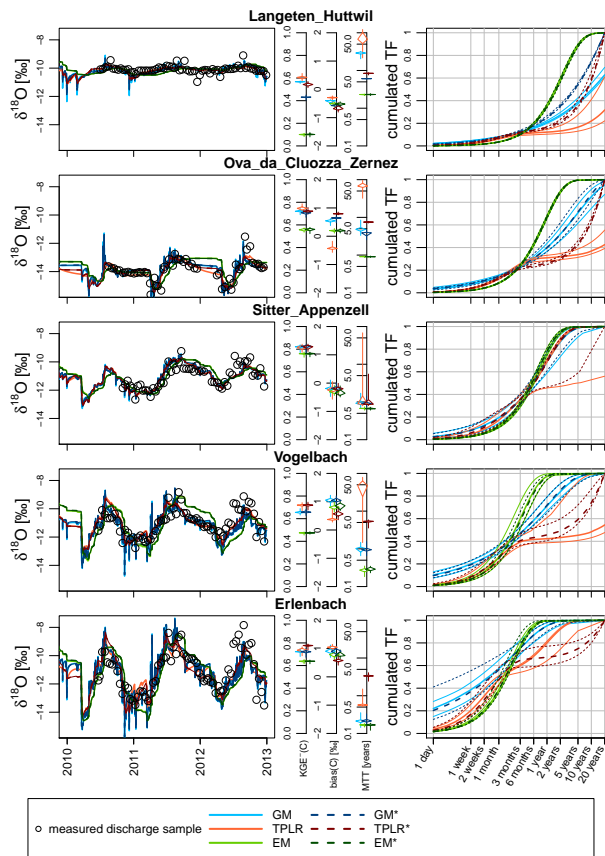


**Figure 5.** Optimisation results for selected catchments. Left: observed and predicted isotope concentrations in discharge. Right: cumulated TTDs (thinner lines indicate ranges of the best solutions). Centre: objective function values for isotopic composition predictions, biases of the predictions and MTTs implied by the optimised TFs; lines indicate the full value range, diamonds the 25 to 75 percentiles of the best solutions.

Title Page

Abstract Introduction

Conclusions References

Tables Figures

◀ ▶

◀ ▶

Back Close

Full Screen / Esc

Printer-friendly Version

Interactive Discussion



## Convolution models revisited

S. Seeger and M. Weiler

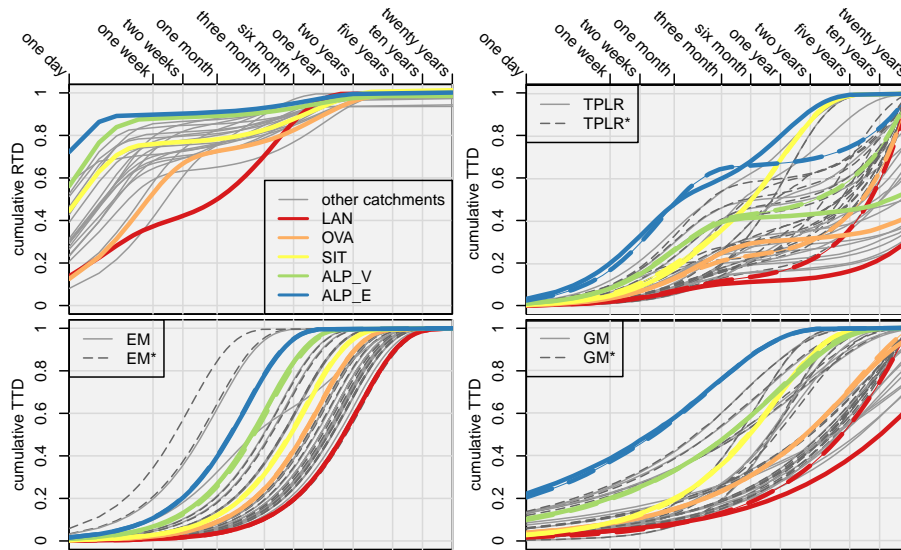


**Figure 6.** Top left: cumulated response time distributions (RTD); bottom left and right column: cumulated transit time distributions (TTD) for different transfer functions. The asterisks (\*) in the legends indicate normalised transfer function variants.

[Title Page](#)

<a href="#">Abstract</a>	<a href="#">Introduction</a>
<a href="#">Conclusions</a>	<a href="#">References</a>
<a href="#">Tables</a>	<a href="#">Figures</a>

⏪
⏩

◀
▶

[Back](#)
[Close](#)

[Full Screen / Esc](#)

[Printer-friendly Version](#)

[Interactive Discussion](#)



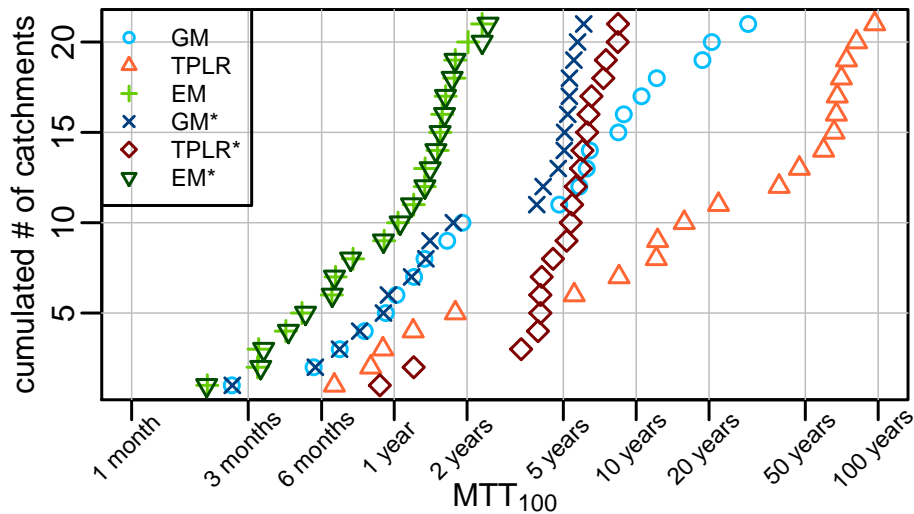


**Figure 7.** Cumulative distribution of catchment mean transit times implied by optimised transfer functions of different types. Normalised transfer function variants are indicated by asterisks.

**Convolution models  
revisited**

S. Seeger and M. Weiler

[Title Page](#)

[Abstract](#) | [Introduction](#)

[Conclusions](#) | [References](#)

[Tables](#) | [Figures](#)

[◀](#) | [▶](#)

[◀](#) | [▶](#)

[Back](#) | [Close](#)

[Full Screen / Esc](#)

[Printer-friendly Version](#)

[Interactive Discussion](#)



## Convolution models revisited

S. Seeger and M. Weiler

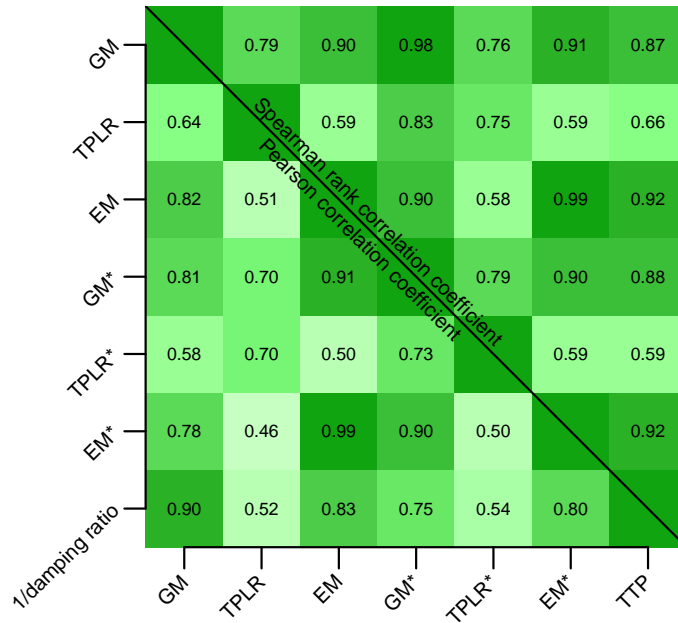


**Figure 8.** Combined matrix of Pearson correlation coefficients (lower left) and Spearman rank correlation coefficients (upper right) for MTTs of all catchments derived by the six different transfer functions and the TTP. Correlation coefficients with  $p$  values  $< 0.005$  are printed in boldface and those with  $p$  values  $\geq 0.05$  are printed in italics.

Title Page

Abstract Introduction

Conclusions References

Tables Figures

⏪ ⏩

⏴ ⏵

Back Close

Full Screen / Esc

Printer-friendly Version

Interactive Discussion



Convolution models  
revisited

S. Seeger and M. Weiler

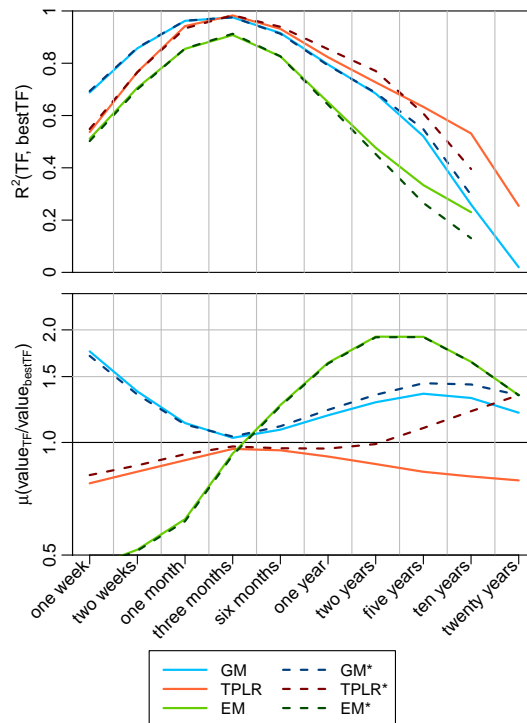


**Figure 9.** Comparison of cumulated discharge fractions after certain elapsed times. Top: correlation coefficients between specific TFs and a selection of the best TFs for each catchment. Bottom: mean value ratios between specific and selected best TFs.

Title Page

Abstract

Introduction

Conclusions

References

Tables

Figures

◀

▶

◀

▶

Back

Close

Full Screen / Esc

Printer-friendly Version

Interactive Discussion



Convolution models  
revisited

S. Seeger and M. Weiler

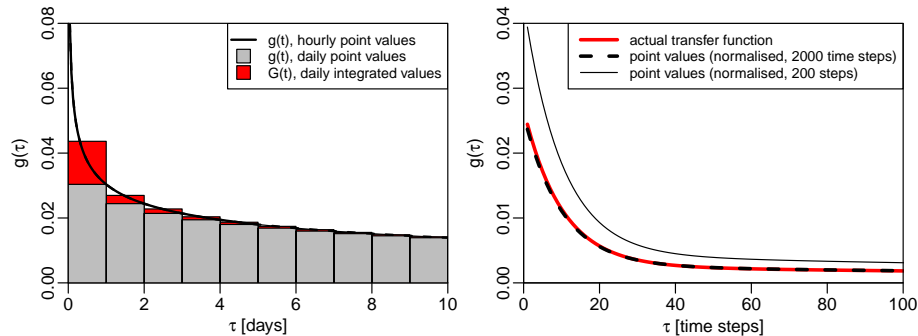


**Figure A1.** Left: Exemplary transfer function values for different computation approaches; right: Exemplary illustration of the effect of transfer function normalization. All three curves are based on a TPLR transfer function with identical parameters. For a long enough modelling time frame (dashed black line), the normalised curve is close to the actual function (red line). For short modelling time frames normalisation leads to considerable distortion (solid black line).

Title Page

Abstract

Introduction

Conclusions

References

Tables

Figures

◀

▶

◀

▶

Back

Close

Full Screen / Esc

Printer-friendly Version

Interactive Discussion



Convolution models  
revisited

S. Seeger and M. Weiler

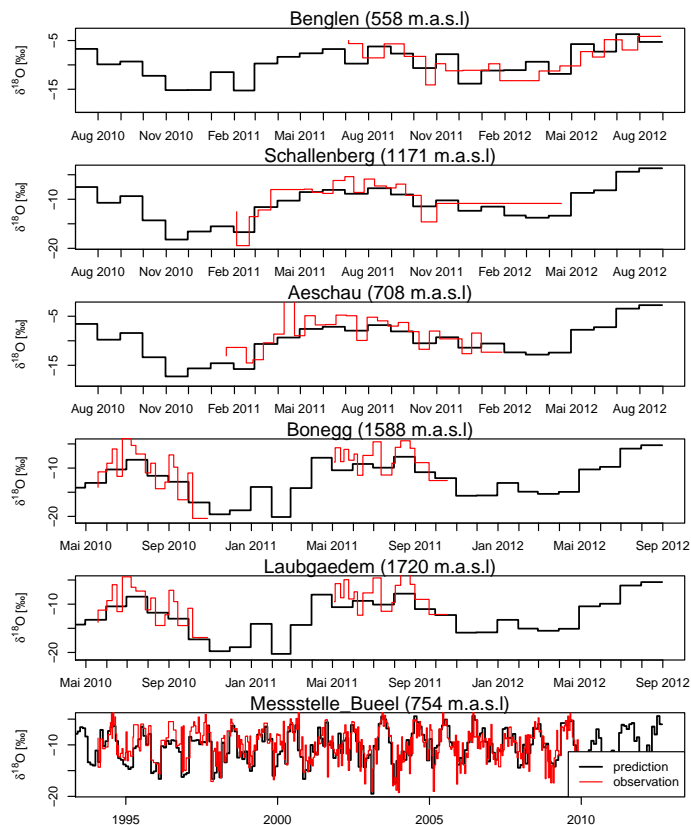


**Figure B1.** Comparison between measured  $\delta^{18}\text{O}$  values (red lines) in precipitation and values obtained by the spatial interpolation method (black lines.)

[Title Page](#)[Abstract](#)[Introduction](#)[Conclusions](#)[References](#)[Tables](#)[Figures](#)[⏪](#)[⏩](#)[◀](#)[▶](#)[Back](#)[Close](#)[Full Screen / Esc](#)[Printer-friendly Version](#)[Interactive Discussion](#)